

**A new installation technology of large diameter deeply-buried caissons  
Practical application and observed performance**

Lai, Fengwen; Liu, Songyu; Li, Yaoliang; Sun, Yanxiao

**DOI**

[10.1016/j.tust.2022.104507](https://doi.org/10.1016/j.tust.2022.104507)

**Publication date**

2022

**Document Version**

Final published version

**Published in**

Tunnelling and Underground Space Technology

**Citation (APA)**

Lai, F., Liu, S., Li, Y., & Sun, Y. (2022). A new installation technology of large diameter deeply-buried caissons: Practical application and observed performance. *Tunnelling and Underground Space Technology*, 125, Article 104507. <https://doi.org/10.1016/j.tust.2022.104507>

**Important note**

To cite this publication, please use the final published version (if applicable).  
Please check the document version above.

**Copyright**

Other than for strictly personal use, it is not permitted to download, forward or distribute the text or part of it, without the consent of the author(s) and/or copyright holder(s), unless the work is under an open content license such as Creative Commons.

**Takedown policy**

Please contact us and provide details if you believe this document breaches copyrights.  
We will remove access to the work immediately and investigate your claim.



## A new installation technology of large diameter deeply-buried caissons: Practical application and observed performance

Fengwen Lai<sup>a,b,c,\*</sup>, Songyu Liu<sup>a,b,\*</sup>, Yaoliang Li<sup>d</sup>, Yanxiao Sun<sup>a,b</sup>

<sup>a</sup> Institute of Geotechnical Engineering, School of Transportation, Southeast University, Nanjing 211189, China

<sup>b</sup> Jiangsu Key Laboratory of Urban Underground Engineering & Environmental Safety, Southeast University, Nanjing 211189, China

<sup>c</sup> Faculty of Civil Engineering and Geosciences, Delft University of Technology, Building 23, Stevinweg 1 / PO-box 5048, 2628 CN Delft / 2600 GA Delft, The Netherlands

<sup>d</sup> Shanghai Foundation Engineering Group Co., Ltd., Shanghai 200002, China

### ARTICLE INFO

#### Keywords:

Large diameter deeply-buried caisson  
Construction technology  
Field observation  
Installation effect  
Interaction

### ABSTRACT

The development of installation technologies of open caissons has been lagging behind increasingly complex construction conditions. For such purpose, a new installation technology of large diameter deeply-buried (LDDB) open caissons has been developed and then used for construction of twin LDDB caissons into undrained ground with stiff soils in Zhenjiang, China. To assess the installation effects and field performance, a monitoring program was presented to document the variations in total jacking forces provided by new shaft driven method, ground water level (GWL) around the caisson shaft, inclination angles of caisson shafts and radial displacements of surrounding soils as well as surface settlements of existing nearby facilities. It is observed that the monitoring data during the installation falls almost entirely within the design criteria, the reported new technology has limited impacts on the induced ground movements, depending on the variation in GWL, interaction between twin caissons and excavation-induced unloading effect. Moreover, the total jacking forces increase approximately in stepwise shape as the installation depth increases; the change law of surface settlements is highly similar to those of GWL, showing their close correlation; the larger inclination angles of caisson shafts are mainly encountered in the earlier installation phase, but well controllable. Further discussion on ground movements caused by various technologies confirms the feasibility of new installation technology. Both the observed and compared results give greater confidence on the use of such the technology in practice.

### 1. Introduction

The rapid expansion of urban population promotes the use of large-scale infrastructure systems, such as bridge foundations, underground space and public works. The evolution of geometric dimensions of some representative infrastructures in recent decades is presented in Fig. 1. It is evidenced that the construction scales of bridge foundations, tunnels, excavations and open caissons continue to enlarge, highlighting the sustained importance of large and deep excavation works. Recently, large diameter deeply-buried (LDDB) open caissons (inner diameter  $D_{in} \geq 15$  m and buried depth  $H \geq 30$  m) are widely used to provide a temporary access to the subsurface for piping and tunnelling, or as permanent works, are utilized for deep foundations, elevators, underground storage, ventilations, pumping stations and sewerage purposes (Dachowski and Kostrzewa, 2017; Fischer et al., 2004; Khasawneh et al., 2017; Lai et al., 2020; Lai et al., 2021; Li et al., 2022; Royston, 2018;

Royston et al., 2016; Schwamb, 2014; Tomlinson and Boorman, 2001). The cross section of caisson shafts can be rectangular or circular. Circular caisson shafts are more mechanically efficient due to the effective resistance to circumferential forces, and also are simpler to construct, which makes it more preferable in practice (Schwamb, 2014). However, compared with the knowledge about rectangular open caissons, the installation effects and field performance of LDDB caissons are little studied.

During the installation, the caisson shaft with cutting edges is progressively sunk into the ground from the surface to a pre-designed depth by excavating the inside soils, either with the aid of its own weight or vertical jacking in a controlled manner. However, this seemingly simple installation process is actually a challenging work for geo-engineers, for instance, the controlling of verticality and penetration-velocity of caisson shafts, as well as the minimization of penetration resistance. Some installation problems, e.g., slowly-sinking, suddenly-sinking, tilting and freezing, are always encountered in the process of caisson installation

\* Corresponding author at: Institute of Geotechnical Engineering, School of Transportation, Southeast University, Nanjing 211189, China.

E-mail addresses: [laifengwen@163.com](mailto:laifengwen@163.com), [F.Lai-1@tudelft.nl](mailto:F.Lai-1@tudelft.nl) (F. Lai), [liusy@seu.edu.cn](mailto:liusy@seu.edu.cn) (S. Liu).

<https://doi.org/10.1016/j.tust.2022.104507>

Received 18 March 2020; Received in revised form 12 November 2021; Accepted 8 April 2022

Available online 15 April 2022

0886-7798/© 2023 The Authors. Published by Elsevier Ltd. This is an open access article under the CC BY license (<http://creativecommons.org/licenses/by/4.0/>).

### Notation

The following symbols are used in this paper:

$c$	Cohesion;
$D_{in}, D$	Inner and external diameters of open caisson;
$e$	Void ratio;
$E_{0.1-0.2}$	Constrained modulus;
$f_{ak}$	Bearing capacity;
$f_s$	Sleeve resistance of CPT;
$F$	Total jacking forces;
GWL	Ground water level
$H$	Penetration depth of caisson;
$K_h, K_v$	Horizontal and vertical permeability coefficients;

$N_{63.5}$	SPT below counts;
$q_c$	Cone resistance of CPT;
$\alpha$	Inclination angle;
$\gamma$	Unit weight;
$\varnothing$	Diameter of jacking pipe;
$\varphi$	Soil friction angle;
$\omega$	Water content;
$\omega_L$	Liquid limit;
$\omega_P$	Plastic limit;
$\delta_v$	Surface settlement of existing nearby facilities;
$\delta_r$	Radial displacements of surrounding soils;
$\delta_{r, \max}, \delta_{v, \max}$	Maximum radial displacement and surface settlement;

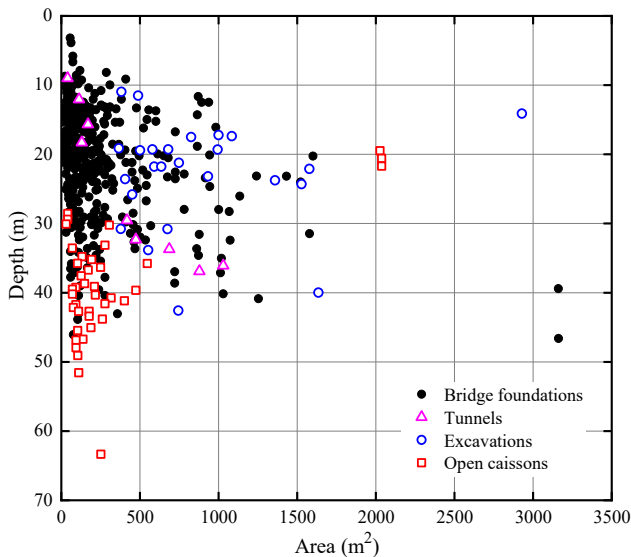


Fig. 1. Variation in geometric dimensions of some representative infrastructures in recent decades [Data from Umeda et al. (2006)].

(Abdrabbo and Gaaver, 2012a). Therefore, the installation controllability needs to be given more attention and further improved. For such purpose, some new caisson installation technologies were reported (Allenby and Kilburn, 2015; Allenby et al., 2009; Newman and Wong, 2011; Peng et al., 2019; Yao et al., 2014), but they were still incompatible with gradually increasing construction scales under complex geological conditions.

To overcome these practical difficulties, the extensive research work, with focuses on installation mechanisms and deformation/displacement characteristics, has been carried out by field observations, laboratory tests, analytical solutions and numerical simulation. Many well-documented case histories of rectangular open caissons (Abdrabbo and Gaaver, 2012b; Hong et al., 2005; Sun et al., 2019; Wong and Kaiser, 1988; Yea and Kim, 2012; Yea et al., 2015; Zhao et al., 2019) were presented to study the mechanical behaviors of caissons during the installation (e.g. skin friction, earth pressure, and spatial stress-state of cutting edges). They indicated that both the skin friction and the earth pressure increase with increasing the caisson depth prior to reaching the maximum values, then decrease gradually due to the stress relaxation near the cutting edges. The similar phenomenon has been observed by some laboratory test results (Chavda et al., 2019; Jiang et al., 2019b; Kumar and Rao, 2010; Zhao et al., 2015). Yea and Kim (2012) presented that the vertical forces acting on the cutting edges of rectangular caissons might be affected by soil properties, shafts' dimension and rigidity,

requiring that geo-engineers made an empirical judgement.

Due to the inaccessible in-situ measurement data for induced ground movements (Belous, 1968; Ho, 2002; Hoffman et al., 2004), a number of numerical works were conducted to further explore the geo-environmental impacts (Georgiannou et al., 2017; Lai et al., 2020; Peng et al., 2011; Sun et al., 2014; Sun et al., 2015). Under the plane strain condition, Peng et al. (2011) established a discontinuous mechanical model incorporated in the finite element (FE) codes for a rectangular open caisson; the computational accuracy of ground movements was dependent on the mechanical boundary conditions (e.g. the imposed skin friction and end-bearing resistance). Georgiannou et al. (2017) used model change method incorporated in PLAXIS 2D&3D to simulate the staged excavation and shaft penetration, but neglecting the kinematic installation process of caisson shaft. The similar problem also emerged in Jiang et al. (2019a). To more realistically study the installation effects, Lai et al. (2020, Lai et al., 2021) introduced the kinematic and continuous 3D numerical techniques with coupling effects between the penetration and excavation, based on the large deformation finite element (LD FE) method and the standard Lagrangian FE method, respectively. However, both techniques are computationally expensive and time-consuming. Some analytical solutions to estimate the ultimate bearing capacity of cutting edges (Solov'ev, 2008; Yan et al., 2011; Royston et al., 2016, Royston et al., 2018, Royston et al., 2021) or earth pressure (Cho et al., 2015; Kim et al., 2013; Liu, 2014; Tobar and Meguid, 2010) on the caisson shafts were thus provided as theoretical basis for numerical simulation. Nevertheless, due to their complexity, the existing analytical solutions were yet constrained to use in practice.

It follows from the aforementioned overview that the current technologies are inefficient for installation of LDDB caissons under complex conditions. It is expected to develop a new installation technology of LDDB caisson installation available in onshore industry under complex conditions. However, previous studies mainly focused on the performance of a single rectangular open caisson; and the more attention was paid to the mechanical behaviors on the caisson shaft and cutting edges (e.g. skin friction, ultimate bearing capacity, lateral earth pressure). Interaction of twin caissons is yet unclear, in particular circular caissons. Moreover, due to the lack of case histories reporting the field performance (e.g. penetration resistances, ground movements, groundwater level, surface settlements of existing facilities) induced by the installation of LDDB caissons, no available measurement data can be used to evidently predict the induced ground movements as well as to reasonably assess the installation effects.

## 2. Objectives and scope of work

The aim of this work is to report a newly developed installation technology of open caissons in undrained ground with stiff soils. The installation of twin LDDB caissons in Zhenjiang, Southeast China was carried out first using this technology. The ground was composed of

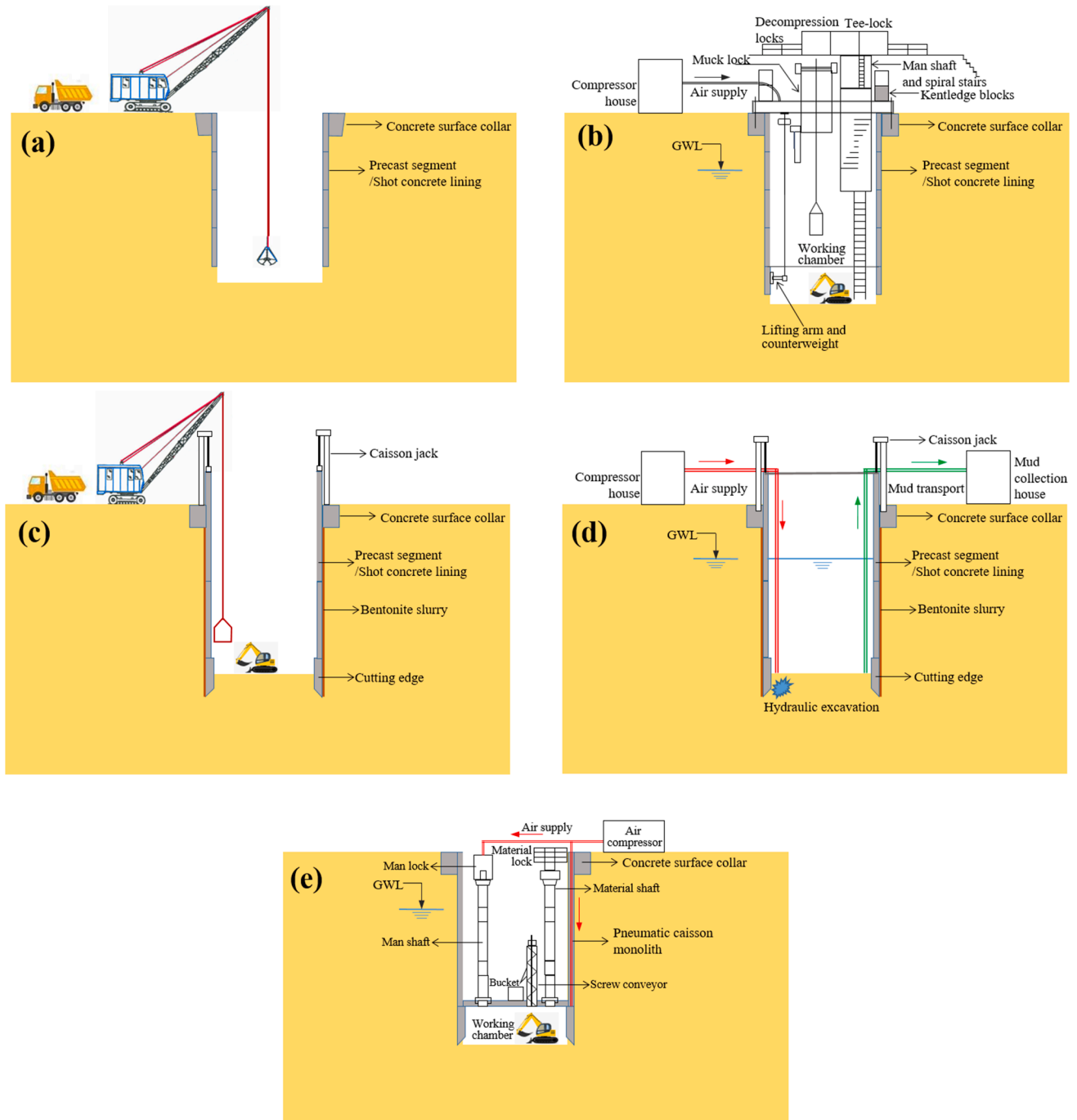


**Fig. 2.** Schematic diagram of current installation technologies: (a) underpinning in free air; (b) underpinning in compressed air; (c) dry open caisson-sinking; (d) wet open caisson-sinking and (e) pneumatic caisson-sinking.

multi-layered soil strata, including the soft soil, sand and stiff clay, etc. During the installation, conventional excavation method was used in the top layers of soft soils for economical purpose. A new excavation method was developed to remove stiff soils at the bottom layers. A new shaft driven method (penetration aid system) was also introduced during the construction to improve the efficiency of caisson penetration. To study the installation effects and field performance caused by the new construction technology, total jacking forces provided by penetration aid system, groundwater level (GWL) around the caisson, inclination angles of caisson shafts, radial displacements of surrounding soils as well as surface settlements of surrounding existing facilities were monitored during the installation process. The discussion on installation effects was finally conducted to explore the use potential (feasibility) of new

installation technology.

### 3. Brief review of current technologies

A number of technologies used for caisson installation have been developed for the use in different environments. The popular ones are underpinning in free air, underpinning in compressed air, pneumatic caisson-sinking, and dry or wet (undrained or drained) open caisson-sinking method. For underpinning in free air method, caisson shafts are sunk into ground by progressively excavating, then installing precast concrete segmental rings with watertight gaskets, or using spray-concrete lining (SCL). It is mostly used in dry and stable ground conditions (Schwamb, 2014; Spagnoli et al., 2017). To avoid the unforeseen



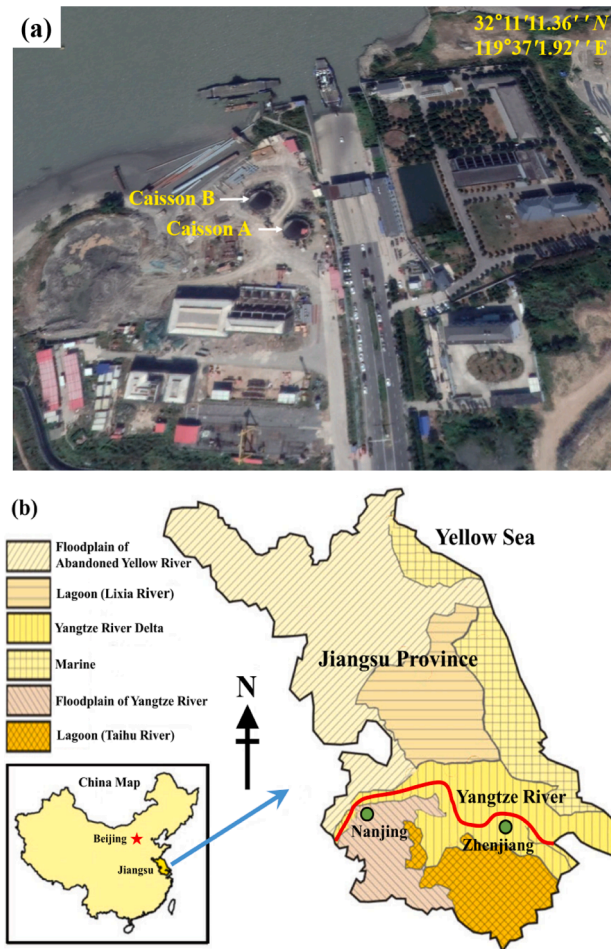


Fig. 3. (a) Location of twin LDDB caissons (map data © 2019 Google, DigitalGlobe); (b) Map in Zhenjiang, China [Adapted by Zou et al. (2017)].

unstable ground conditions, underpinning in compressed air method is used to balance the earth pressure and artesian pressure (Allenby and Kilburn, 2015). In pneumatic caisson-sinking method, the working chamber air pressure can be controlled to balance the external hydrostatic pressure and stabilize weak floor strata, thus soil can be excavated in a dry chamber. In this method, a shaft structure can be progressively sunk in a controlled manner in low strength soils (Dhinian, 2003). However, both for unpinning method and pneumatic caisson-sinking method under the compressed air environment, workers unavoidably suffer from caisson sickness when entering such the working chamber.

Dry or wet open caisson-sinking method can be used in the drained or undrained conditions respectively, depending on the surrounding environment. Using this method, a shaft structure can be progressively sunk into drained (dry) or undrained (wet) ground either under its own weight or using controlled caisson jacks. Nonetheless, the method is generally not suitable in ground with very stiff or hard clays as it is hard for the penetration of the cutting edge. More details of various installation technologies presented here can be seen in Fig. 2.

Owing to versatility of operational conditions, open caisson-sinking method has been more recommended by geo-engineers to use in practice. Different excavation methods and shaft driven methods have been developed (Allenby and Kilburn, 2015; Allenby et al., 2009; Bolyachevskii and Chumakov, 1975; Maslik et al., 1978; Morrison et al., 2004; Newman and Wong, 2011; Sheil et al., 2018; Verstov et al., 2019; Zheng et al., 2019). Grab bucket is the most common tool used for excavation. But it is not suitable in wet condition, in particular when the groundwater table is high. Air suction method is often used to excavate and remove soils in wet and soft ground, nonetheless with lower efficiency.

Therefore, there is a lack of efficient installation method in undrained ground with stiff clays.

To overcome above shortcomings, Shanghai Foundation Engineering Group Co., Ltd developed a new, automatic and intellectual installation technology of LDDB caissons. This technology was attempted to use in the undrained stiff ground under complex environments. Here the auxiliary penetration measure was a combination of slurry lubrication and vertical jacking method. The more detailed descriptions to this new technology will be given below.

## 4. Background

### 4.1. Project description

The twin LDDB caissons, with the same configuration, were constructed as drinking water wells located in Zhenjiang (32° 11' N and 119° 37' E), China, by the bank of the Yangtze River (Fig. 3). The existing nearby facilities on the site were Jiangxin Wharf, Zhuzhao Road, flood walls and a three-story building (Fig. 4). During the construction, Caisson A (denoted as CA) was first installed, followed by Caisson B (defined as CB), but the interval was short.

As shown in Fig. 4, the horizontal spacing of twin caissons was 15 m. CB was 15 m away from the Yangtze River bank. The distance between CA and Zhuzhao Road was equally 15 m. Fig. 5 presents the cross section of twin LDDB caissons. The designed penetration depth ( $H$ ) of each caisson was 38.5 m below ground surface (BGS) into the stiff clay layer. The internal diameter of each caisson ( $D_{in}$ ) was 15 m. The height of the caisson shaft with concrete cutting edges was 41.2 m. Each caisson was composed of six shaft segments, and was installed in three phases: Phase 1 (P1, bottom section): formed with two pieces of 6.4 m (height)  $\times$  1.3 m (thickness) segments; Phase 2 (P2, middle section): one piece of 6.8 m  $\times$  1.1 m and one piece 7.2 m  $\times$  1.1 m segment, and Phase 3 (P3, top section): two pieces of 7.2 m  $\times$  0.9 m segments. Prior to the each installation phase, the connection work between two segments of concrete linings needed to be carried out to produce a continuous caisson shaft, therefore the corresponding heights of three continuous shafts were 12.8 m, 14.0 m and 14.4 m, respectively. The penetration depths in three installation phases were 11.8 m BGS, 25.8 m BGS and 38.5 m BGS, respectively. The antifricition steps with the height of 0.2 m were set at the connections amongst three sections for reducing the skin friction. Moreover, two holes were pre-casted on prescribed segments to form an entrance for pipelines on the shaft at the depth of 30.5 m BGS (1.8 m diameter) and 9.3 m BGS (2.2 m diameter).

### 4.2. Ground condition

The elevation at the site ranged from 2.44 m to 5.38 m, according to the Yellow Sea Height Datum. Subsoil at the site was comprised of Quaternary deposits. The ground profile was composed of six layers, including fill, very soft clay, silty sand, silty clay with sand, stiff clay and strongly weathered granite layer, as shown in Fig. 6. The silty sand layer formed a confined aquifer. The ground water level ranged from 0.5 m to 3.0 m (with an average of 2 m) below the ground surface with the variation of seasonal water supply. When the construction finished, the ground surface was backfilled at a height of 2.4 m.

Prior to the construction, geotechnical investigations, including a series of laboratory tests for the Shelby tube soil samples (e.g., consolidation, direct shear, triaxial, and seepage analysis tests) and in-situ tests (e.g., standard penetration tests (SPT) and cone penetration tests (CPT)), were carried out to determine soil profiles along with measured soil parameters at the site, as depicted in Fig. 6. The soil unit weight ( $\gamma$ ) was measured by ring shear tests; the water content ( $\omega$ ) was obtained by oven-drying method, and the liquid limit ( $\omega_L$ ) and plastic limit ( $\omega_P$ ) were derived by photoelectric liquid-plastic testers; the cohesion ( $c$ ) and soil friction angle ( $\phi$ ) were deduced from consolidated undrained direct shear (CUDS) tests; the void ratio ( $e$ ) and constrained modulus ( $E_{0.1-0.2}$ )



Fig. 4. Bird view of twin LDDB caissons (After Lai et al., 2021).

were determined according to one-dimensional compression (oedometer) tests; the horizontal and vertical permeability coefficients ( $K_h$  and  $K_v$ ) were obtained by laboratory constant head permeability tests. Furthermore, in-situ testing results around caissons, including SPT blow counts ( $N_{63.5}$ ), CPT cone resistance ( $q_c$ ) and CPT sleeve resistance ( $f_s$ ), were also shown in Fig. 6. Both the laboratory testing and the in-situ testing results indicated that the second layer was the very soft saturated clay with creep behavior; the fifth layer was the very stiff soil so-called Yangtze River Delta clay with very high cohesion ( $c$ ) of 92 kPa and friction angle ( $\varphi$ ) of  $17.6^\circ$ , and the bearing capacity of which ( $f_{ak}$ ) was 260 kPa, as shown in Fig. 7.

#### 4.3. Main focuses

For the installation implementation, caisson shafts needed to be safeguarded, and the excavation stability also needed to be guaranteed during the installation, thus the interaction between twin LDDB caissons required a reasonable solution. However, due to the construction interval and the small horizontal spacing between the twin LDDB caissons, the interaction effect is obvious, showing the change in verticality of caisson shafts (i.e. inclination angle  $\alpha$ ), GWL around the caisson and radial displacements of surrounding soils ( $\delta_r$ ) and surface settlements of existing facilities ( $\delta_v$ ). In accordance with the design criteria of caisson installation, the inclination angle of caisson shafts during the installation requires to be lower than  $\pm 6^\circ$  (SMEDI (2015)) and the surface settlement of existing facilities requires be less than 0.15% excavation depth of the LDDB caisson (MOHURD, 2011).

#### 5. New installation technology

Fig. 8 gives the diagrammatic sketch of the construction equipment

of new LDDB caisson installation technology. It mainly consists of mud rushing and sucking system, stiff soil breaking system, penetration aid system, floating operation platform, excavation base detecting instrument and programmable logic controller (PLC). In the caisson, the operation platform can be freely rotated by twin gyros to ensure the excavations in all directions. The excavation is undertaken mainly combining stiff soil breaking system (i.e., two moveable drilling pipes along sliding tracks) with mud rushing and sucking system. In this process, the excavation base detecting instrument was employed to observe the excavation base in deep water. Meanwhile, new penetration aid system controlled by PLC is used to provide additional vertical jacking forces. It is noted that PLC can be also documented the jacking force of each hydraulic jack and total jacking force of the whole system.

The operation mechanisms of the new installation technology can be divided into undrained excavation in the ground and caisson shaft sinking. Fig. 9 describes the operation mechanisms of the excavation in undrained stiff clays. Before the caisson penetrates into stiff clays, the floating operation platform requires to be first installed at the groundwater table inside the caisson. Subsequently, stiff soil breaking system, composed of two steel drilling pipes for injection of ultra-high pressure water, is employed to break soils in deep water. Broken soils would be transferred as muds, then suck into mudding pipes under the air suction, finally discharged into slurry ponds.

For the caisson shaft driven in stiff soils, in addition to lubrication of bentonite slurry sleeve, a new shaft driven method (i.e. penetration aid system) is used to provide the vertical jacking force. Fig. 10(a-e) give the detailed operation mechanisms of new penetration aid system. First, in light of caisson diameter, the precast steel counterweight plates are placed around the caisson for anti-uplift. An even number of jacks are then installed on the surface collar [see Fig. 10(a)]. As shown in Fig. 10 (b-d), the required jacking forces are provided by hydraulic jacks, the



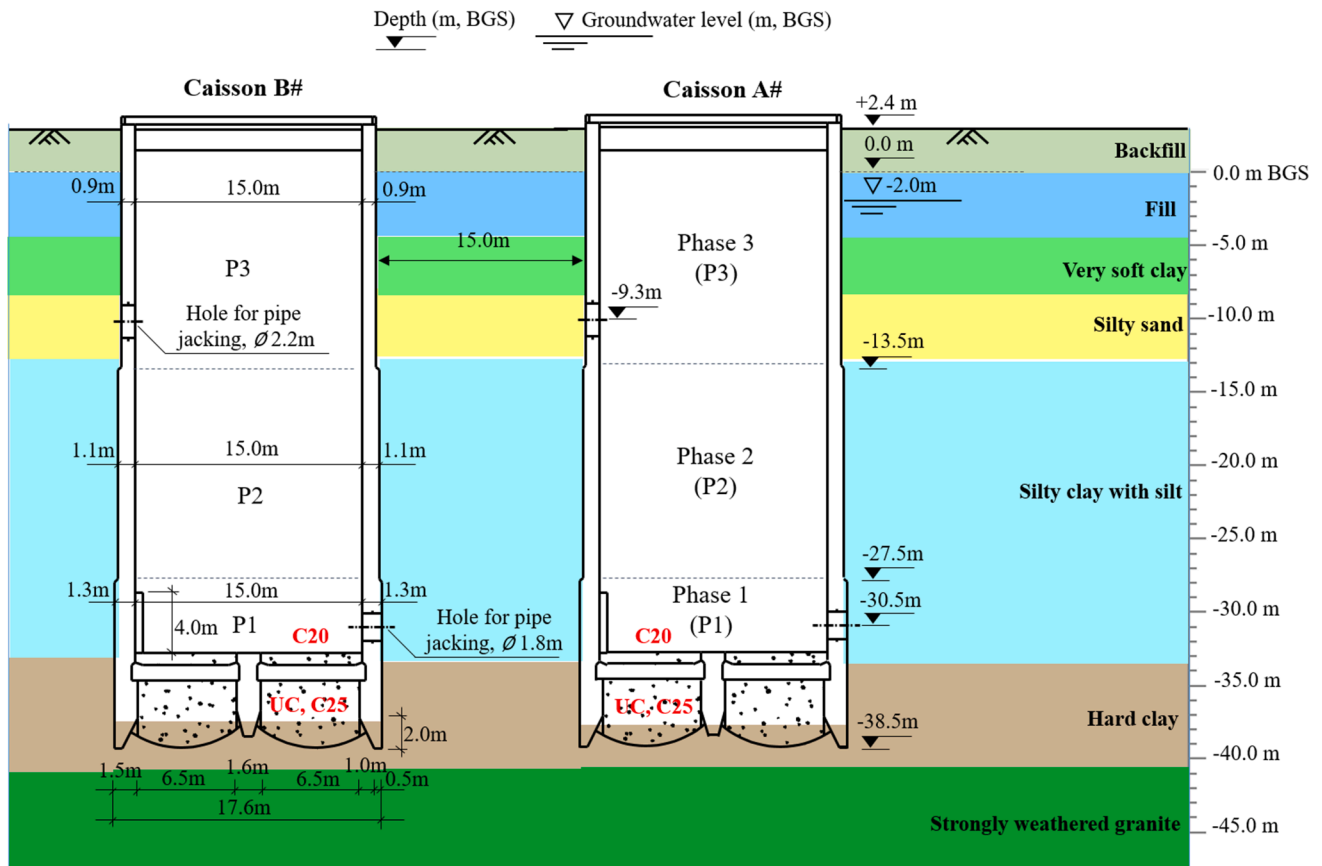


Fig. 5. Profiles of twin LDDB caissons.

generated reaction forces are transmitted by multiple steel stranded wires. The reaction forces can be then balanced by the surface collar and counterweight plates. As the penetration resistance increases, the number of counterweight plates is required to be increased for balance. Such cyclic process of jacking and retracting of hydraulic jacks finally promotes the LDDB caisson installed to a designed depth in stiff soils. The application of penetration aid system during the installation of the LDDB caisson can be seen in Fig. 10(e). It is worth noting that the system can use the PLC to automatically control the cyclic process of jacking and retracting of each hydraulic jack. Therefore, it can well avoid the non-uniformity of jacking forces, which is beneficial for the control of verticality of caisson shafts and the reduction of ground movements, also strengthening the construction controllability. Furthermore, the induced geoenvironmental impacts can be significantly lowered using this system because of the existence of a certain height of soil plugging (about 2–2.5 m) inside the caisson.

## 6. Installation process

As shown in Figs. 5 and 6, around the top 13 m of soils are fill materials, very soft clay and silty sand. The thickness of these three layers is about the same height (12.8 m) of the bottom section of the caisson. During the installation of this section in Phase 1, open caisson-sinking method was used considering the soil condition. Crab bucket was used to remove soft soils, and shaft segments were sunk into the ground under their own weight, as shown in Fig. 11. Once the shaft reached the silty clay layer, the resistance to the shaft increases, and it became harder for shaft segments to penetration under their own weight.

For the middle section in Phase 2, new penetration aid system was installed to provide downward driven forces to the shaft as shown in Fig. 10. In this phase, the removal of soils using crab bucket became harder and un-economical with high water table in the caisson. Thus,

traditional air suction method was used to remove the sandy silt soil, as shown in Fig. 12. Upon finishing the driven of section 2, the tip of the shaft was at the depth of 25.8 m below the ground surface, which is still in the silty clay layer.

For the top section in Phase 3, to further improve the soil-removal efficiency and make the caisson shaft driven in stiff clays, a novel undrained excavation method was proposed during the installation of the top section, as shown in Fig. 13. Once soils inside the caisson were removed completely, underground concrete was pumped into the bottom of the caisson to form a plug as the base for water retention. The thickness of the concrete base is 4.5 m with a cross beam at the depth of 34.5 m (see Fig. 5).

The two caissons were installed almost simultaneously, with CA being launched on the 6th of April, and CB on the 20th of April 2017. The whole installation process lasted 238 days for CA and 273 days for CB. A detailed schedule is illustrated in Fig. 14. From the schedule, we can see that the majority of time was spent on casting shaft segments and preparation for installation. The actual days for the installation, including soil excavation and shaft driven, of each section are 15, 23 and 28 days for CA and 10, 25 and 38 days for CB. The preparation time (not including casting shaft segments) for the installation of each section is 7, 3 and 14 days for CA, and 7, 7, and 27 days for CB. The schedule shows that as the caissons get deeper, the installation process takes longer. Also to minimize the interaction between the two caissons, the installation of the shaft segments was performed in alternative sequences, i.e., the segments in CB were installed during the fabrication of shaft segments of CA, and vice versa.

## 7. Instrumentation

During the installation of twin LDDB caissons, a comprehensive field instrumentation program was carried out to monitor the total jacking

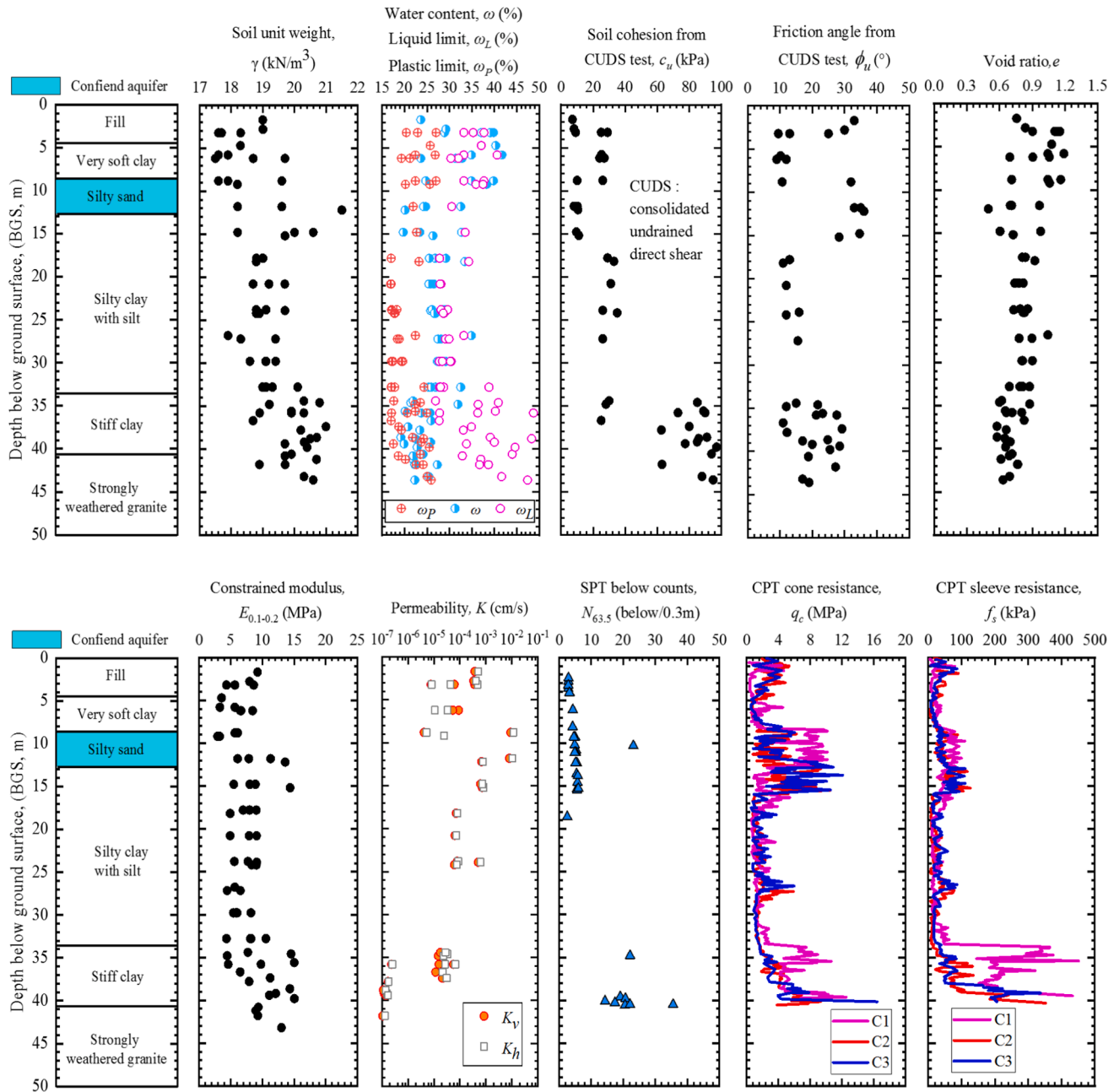
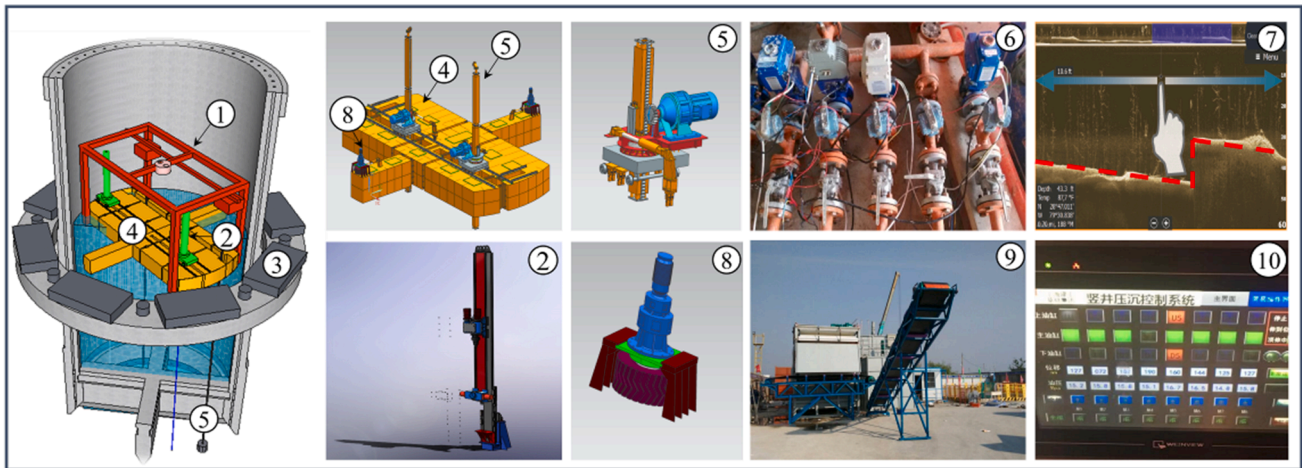


Fig. 6. Soil profiles along with the measured soil properties at the site (After Lai et al., 2021).



Fig. 7. Very stiff soils called Yangtze River delta clays (Images by Dagang waterworks project team).



1. Hoisting equipment for mud rushing and sucking system
2. Stiff soil breaking system
3. Penetration aid system
4. Floating operation platform
5. Mud rushing and sucking system
6. Antifriction system
7. Excavation base detecting instrument
8. Gyro
9. Slurry-residue soil separation system
10. Programmable logic controller (PLC)

Fig. 8. Diagrammatic sketch of new construction equipment of new installation technology.

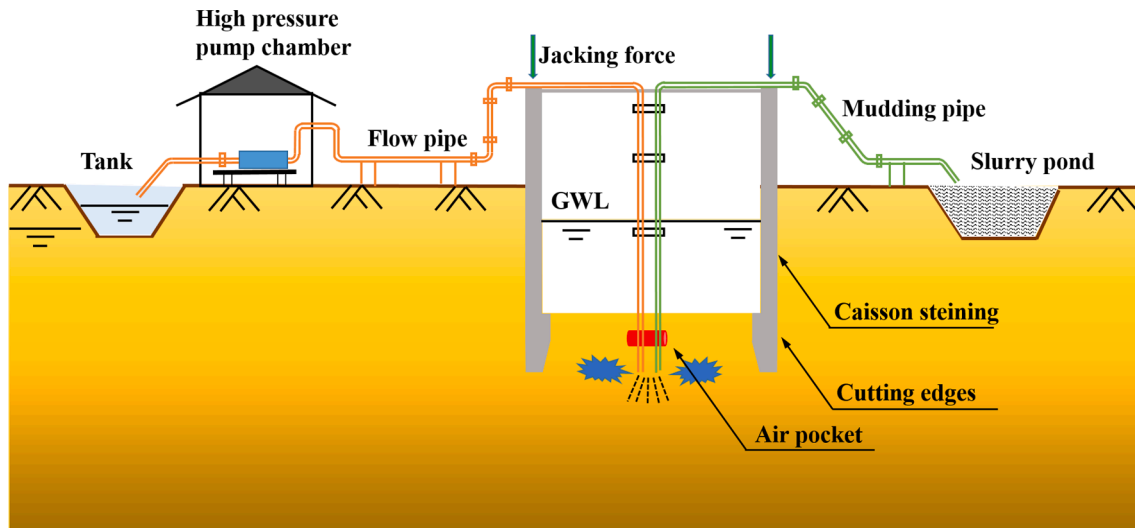


Fig. 9. Operation mechanisms of the excavation in undrained soils using new open caisson installation technology.

force provided by new penetration aid system ( $F$ ), GWL around the caissons, inclination angles of caisson shafts ( $\alpha$ ), and radial displacements of soils ( $\delta_r$ ) around the caissons as well as surface settlement and heave of existing buildings and flood walls ( $\delta_v$ ). In the monitoring program, we used inclinometers and extensometers to measure the radial soil displacement and the vertical settlement, respectively. The inclination angle can be observed and calculated by the elevation difference of measurement points on the caisson top, as indicated below. The total jacking force can be directly read on the screen of PLC as the load cells have been installed within the jack and then documented by PLC.

All the key monitoring points are plotted in Fig. 15. Unfortunately, ground settlements induced by installation of twin LDDB caissons were inaccessible as the monitoring cells have been damaged by surrounding vehicles. Therefore, surface settlements of surrounding existing facilities were required to be precisely measured, to control ground settlements resulting from the installation of twin LDDB caissons.

In the field-monitoring program, 16 observation points, including

F1-F3 for the surrounding flood walls and S1-S13 for the existing buildings, were set up to measure the surface settlements. For the surface settlement, the positive values indicated subsidence, and the negative values indicated uplift. Six inclinometers (R1-R6) were installed, at a radial distance ( $x$ ) of 5 m ( $x/D_{in} = 0.333$ ) from the caisson shaft, to monitor the radial displacements. The measured values of  $\delta_r$  were considered positive when towards the centerline of adjacent caisson shaft and negative when away from adjacent on. To ensure the installation controllability, the verticality of caisson shafts and variation in GWL were also monitored. Eight observation points (A1-A4 and B1-B4) were respectively set on the top of twin LDDB caissons to measure their elevation, further converting the inclination angles of caisson shafts in the same vertical plane based on the arctangent function of the ratio of the elevation difference to the external diameter. The positive value of  $\alpha$  represented that the caisson shaft was tilting to the direction of A1, A2, B1 or B2, and the negative value represented that the shaft was tilting to the direction of A3, A4, B3 or B4. Two monitoring points



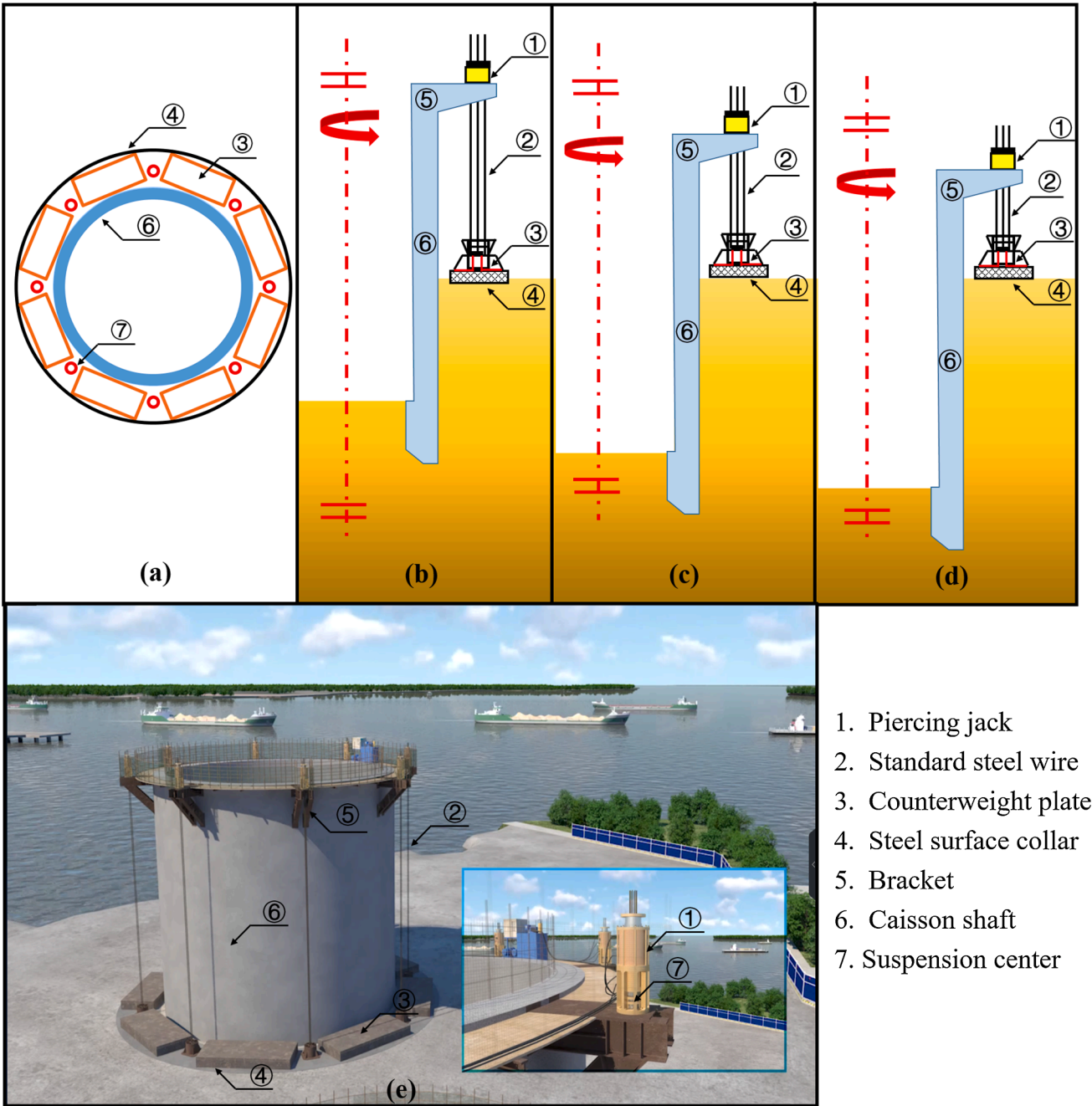


Fig. 10. Operation mechanisms of new penetration aid system in the developed installation technology.

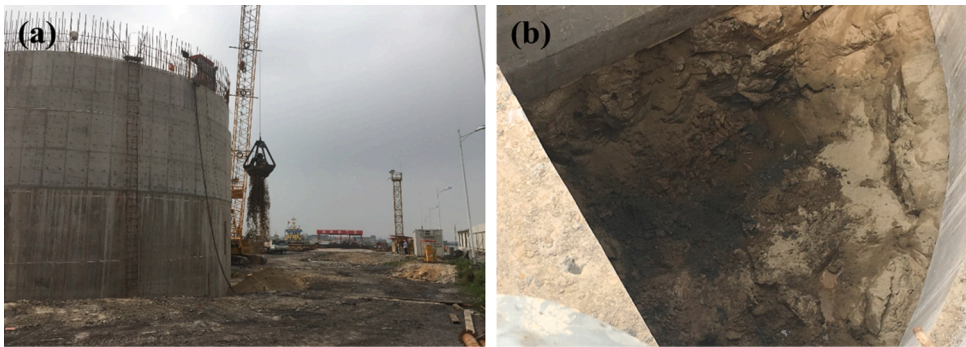


Fig. 11. Installation Phase 1: crab bucket method (Images by Dagang waterworks project team).



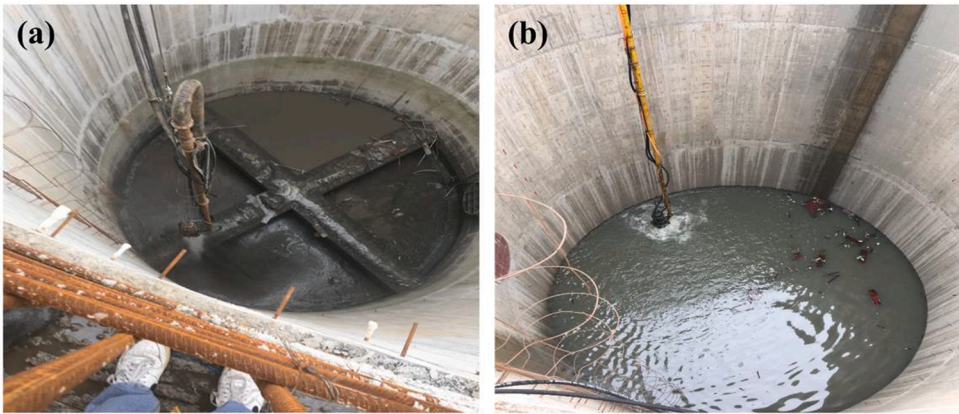


Fig. 12. Installation Phase 2: air suction method (Images by Dagang waterworks project team).

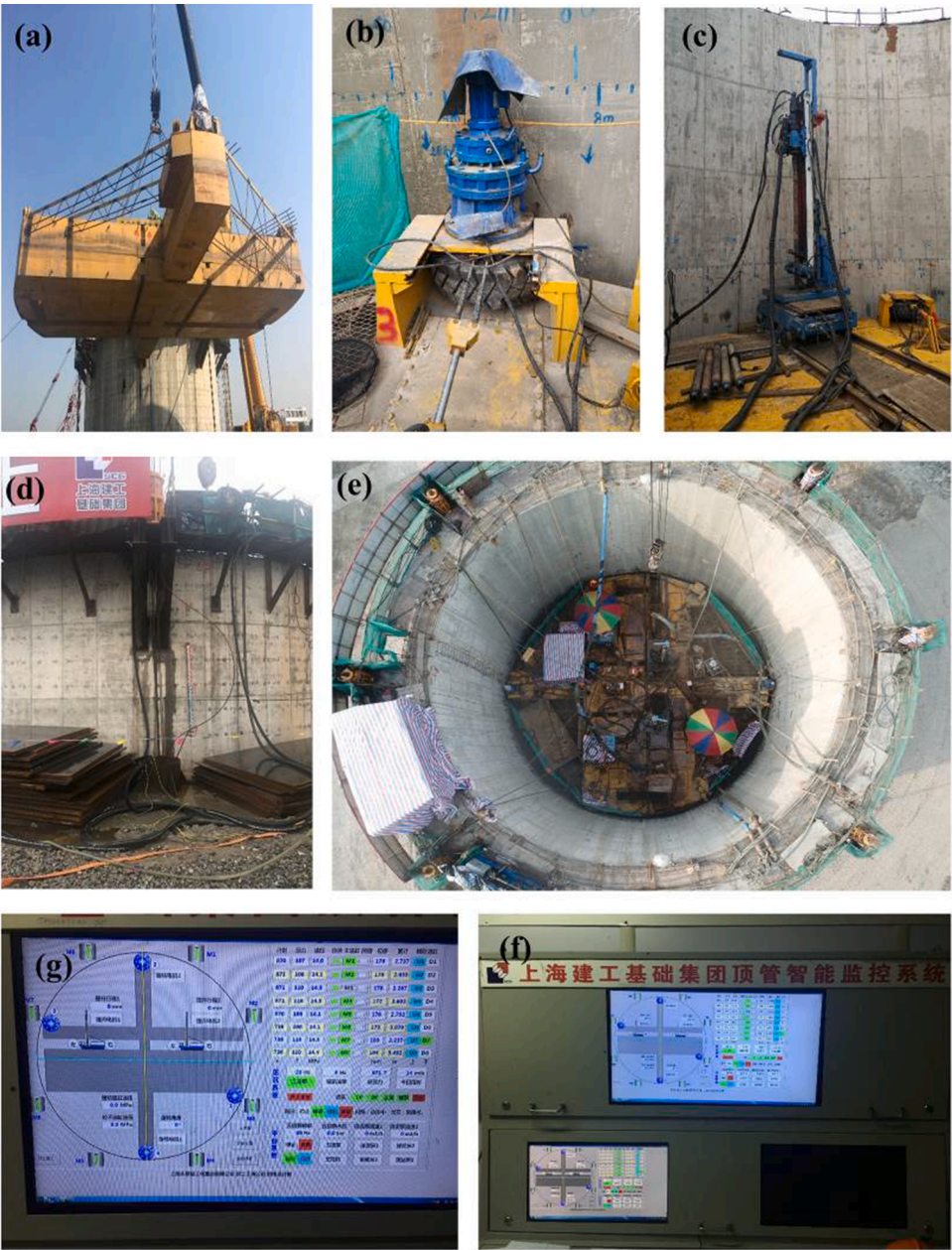


Fig. 13. Installation Phase 3: new installation technology (Images by Dagang waterworks project).

Actual Project Stages				Calendar Plan											
Tasks	Start data	End data	Duration	Apr.	May	Jun.	Jul.	Aug.	Sept.	Oct.	Nov.	Dec.	Jan.		
Caisson A installation ( $D=17.6\text{m}$ , $H=38.5\text{m}$ )	4/6/2017	11/29/2017	238 days												
Site preparation	4/6/2017	4/8/2017	3 days												
Installation of anchor piles, brick templates and scaffolds	4/9/2017	4/23/2017	15 days												
Fabrication of the shaft segments for Phase 1	4/24/2017	6/12/2017	50 days												
Preparation for caisson A installation in Phase 1	6/13/2017	6/19/2017	7 days												
Penetration to 11.8m BGS in Phase 1	6/20/2017	7/4/2017	15 days												
Fabrication of the shaft segments for Phase 2	7/5/2017	8/13/2017	40 days												
Preparation for caisson A installation in Phase 2	8/14/2017	8/16/2017	3 days												
Penetration to 25.8m BGS in Phase 2	8/17/2017	9/8/2017	23 days												
Fabrication of the shaft segments for Phase 3	9/9/2017	10/18/2017	40 days												
Preparation for caisson A installation in Phase 3	10/19/2017	11/1/2017	14 days												
Penetration to 38.5m BGS in Phase 3	11/2/2017	11/29/2017	28 days												
Caisson B installation ( $D=17.6\text{m}$ , $H=38.5\text{m}$ )	4/20/2017	1/17/2018	273 days												
Site preparation	4/20/2017	4/22/2017	3 days												
Installation of anchor piles, brick templates and scaffolds	4/23/2017	5/8/2017	15 days												
Fabrication of the shaft segments for Phase 1	5/9/2017	6/27/2017	50 days												
Preparation for caisson A installation in Phase 1	6/28/2017	7/5/2017	7 days												
Penetration to 11.8m BGS in Phase 1	7/6/2017	7/15/2017	10 days												
Fabrication of the shaft segments for Phase 2	7/16/2017	9/1/2017	48 days												
Preparation for caisson A installation in Phase 2	9/2/2017	9/8/2017	7 days												
Penetration to 25.8m BGS in Phase 2	9/9/2017	10/3/2017	25 days												
Fabrication of the shaft segments for Phase 3	10/4/2017	11/12/2017	40 days												
Preparation for caisson A installation in Phase 2	11/13/2017	12/9/2017	27 days												
Penetration to 38.5m BGS in Phase 3	12/10/2017	1/17/2018	38 days												

Fig. 14. Schedule of construction activities during the installation of twin LDDB caissons.

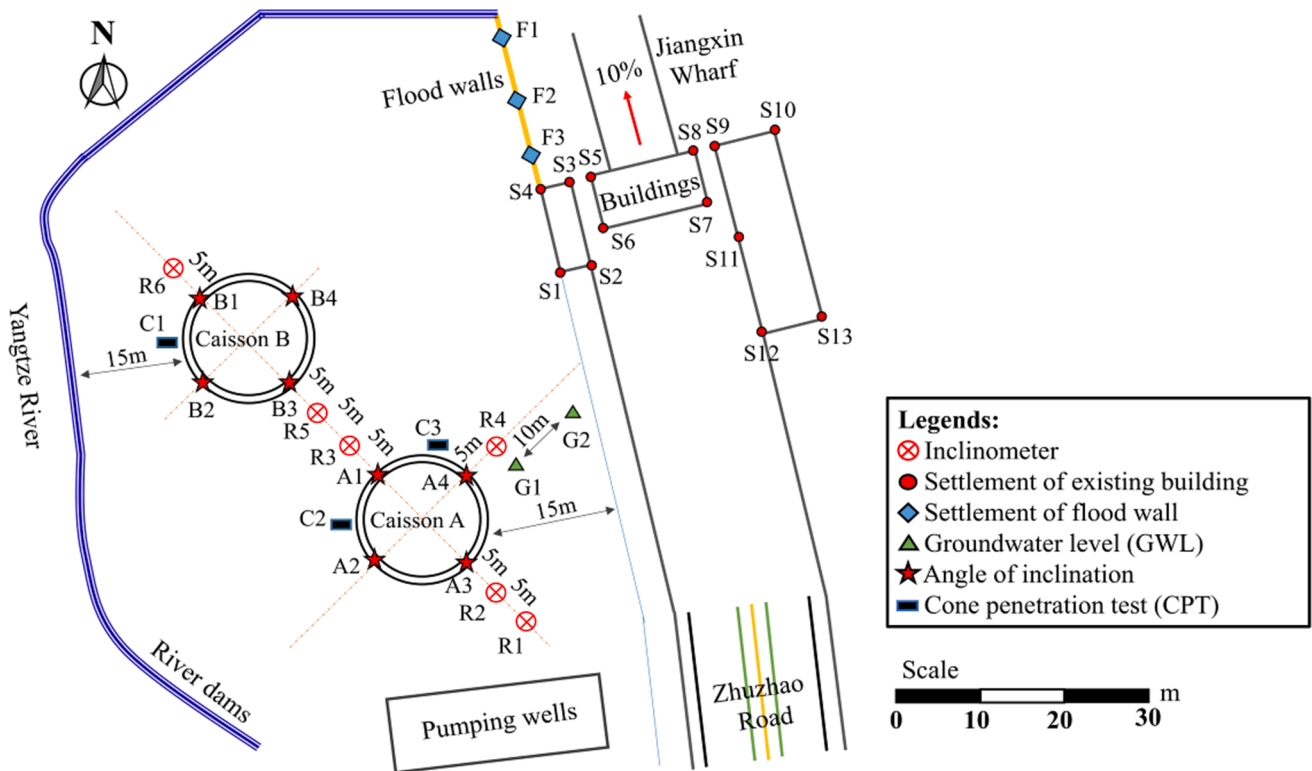


Fig. 15. Layout of the key monitoring points.

(G1 and G2), 5 m and 15 m away from Caisson A, were fixed for observing the daily variation in GWL. In addition, C1-C3 were the in-situ testing points for conducting CPTs to describe the more geological information.

## 8. Observed performance

### 8.1. Total jacking forces

Fig. 16 shows the relationship between total jacking forces ( $F$ ) provided by penetration aid system and penetration depth ( $H$ ) of twin LDDB caissons. It can be found that both Caissons A and B follow approximately ladder-increasing relationship between  $F$  and  $H$ . This indicates that the vertical penetration resistance, composed of end-bearing, skin



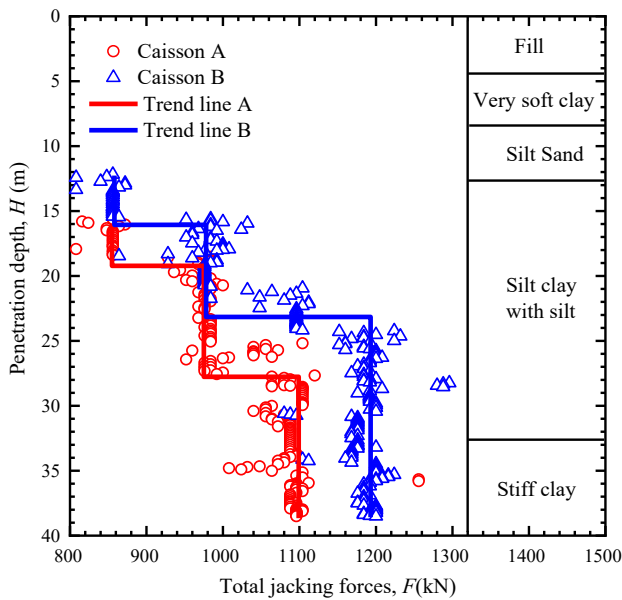


Fig. 16. Relationships correlating the total jacking forces and penetration depth of LDDB caissons.

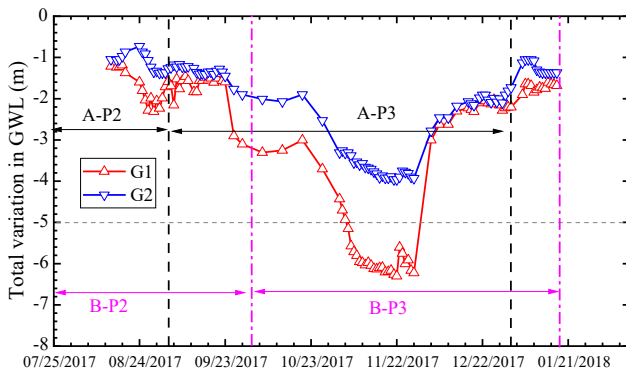


Fig. 17. Variation in GWL during the installation of twin LDDB caissons.

friction and buoyancy, remains basically the constant in the same soil layer. It is concluded that the penetration resistance is mainly depended on end-bearing on the cutting edge embedded into a specific soil layer, and the skin friction is relatively smaller than end-bearing due to use of bentonite slurry lubrication.

During the installation, to reduce the vertical penetration resistance, more bentonite slurry was injected for lubrication for the later-installed CB. However, comparing to CA, the  $F$  value of CB is instead larger. This phenomenon might be explained as following. The installation activities of CA (prior to CB) resulted in the soil compaction effect to redistribute soil stresses. Therefore, the soils' strength around CB slightly increased, in particular deep ground, causing the increased vertical jacking resistance. This also implies that during the installation of twin LDDB caissons, geo-engineers should pay greater attention to the construction controllability of the later-installed caisson.

## 8.2. Groundwater level (GWL)

The controlling in groundwater level (GWL) plays a significant role in the safety and stability of LDDB caissons installed in soils. Note that the recharge of groundwater is achieved by stiff soil breaking system (injecting high-pressure water), and the pumping of ground water is achieved by mud rushing and sucking system (removing broken soil).

Fig. 17 plot the daily variation in GWL during the installation of twin

LDDB caissons. In Fig. 17, some interesting phenomena can be found as following: the values of GWL at G1 and G2 are slightly varied in Phase 2 of twin LDDB caissons; while in Phase 3, the value of GWL at G1 first decreases to  $-5\text{m}$  and that of G2 reduces to  $-3\text{m}$  in earlier stage, then they both maintain a steady state, but recover fleetly to initial values in the later phase. Overall, the total variation in GWL at G1 is about within the range of  $0\text{ m}$  to  $-3\text{m}$ , and that at G2 is about within the range of  $0\text{ m}$  to  $-5\text{m}$ .

The variation in GWL is closely related to the operational characteristics of the developed new installation technology. The slight changes in GWL in Phase 2 may be due to morning and evening tide of Yangtze River that are in the range of  $0\text{ m}$  to  $-1\text{m}$ . The variations in GWL at G1 and G2 in Phase 3 may be explained as following: (1) In the earlier stage, the effect of stress relaxation near the cutting edges and seepage or groundwater inflow on the stability of caisson shaft can be neglected because of the existence of inside soil plugging with a height of  $2\text{ m}$ . The reasonable and allowable drawdown inside the caisson that is achieved by mud rushing and sucking system, similar to a pumping well, can be thus contributed to decreasing the required driving force due to the reduction of buoyancy. This also leads to the formation of groundwater depression cones around LDDB caisson shafts. (2) The phenomena of slow sinking and freezing will occur as installation process advances and LDDB caissons are sunk into the stiff clays, causing a short construction suspension. Therefore, the relatively stable GWL can be apparently observed during this period. (3) To fully fail and break stiff clays, it requires stiff soil breaking system to inject more high-pressure water, similar to recharge wells, leading to that the GWL at G1 and G2 gradually recover to the initial values.

## 8.3. Inclination angles

Fig. 18(a and b) present the variation of  $\alpha$  of Caissons A and B in two perpendicular orientations (Fig. 15) during the whole installation process. It can be clearly seen from the figure that the values of  $\alpha$  are in the range of  $-0.5^\circ$  to  $0.5^\circ$  for both CA and CB. Maximum values ( $\alpha_{\max}$ ) of inclination angles of CA are  $0.456^\circ$  in A1-A3 orientation and  $0.498^\circ$  in A2-A4 orientation, respectively; and those of CB are  $-0.267^\circ$  in B1-B3 orientation and  $0.487^\circ$  in B2-B4 orientation. Moreover, all these values are within the design criteria of  $\pm 6^\circ$  suggested by SMEDI, implying that the developed new installation technology can better control the verticality of caisson shafts. It is also noted that, for deeper penetration, under the interaction, both caissons incline toward the bank of the Yangtze River (i.e. toward the A1-A2 and B1-B2) where the soil properties are weaker than onshore due to scours.

The further examination on the measured values of  $\alpha_{\max}$  shows that, the relatively obvious inclinations of caisson shafts occur in the earlier installation stage (P1), but such the obvious inclination gradually mitigates as the LDDB caisson installation enters into Phase 2. This is because the caisson shaft with the lighter weight in the earlier installation stage is more affected by excavation actives. In all, to attain the successful installation of LDDB caissons, the remedial deviation-correcting measures must be timely took to adjust the verticality when encountering the larger inclination angle of shafts, in particular the earlier stage of the installation.

## 8.4. Radial displacements

Fig. 19(a-f) present the measured radial displacements ( $\delta_r$ ) of surrounding soils along the caisson shaft at R1, R2, R3, R4, R5 and R6 induced by the installation of twin LDDB caissons, respectively. At R1 that is  $10\text{ m}$  away from CA, the soils are mainly subjected to unloading effect caused by the excavations of CA and CB, showing the traditional cantilever-shaped displacement mode similar to that of the rigid cantilever diaphragm walls in excavation systems [see Fig. 19(a)]. Namely, the value of  $\delta_r$  gradually decreases along the caisson shaft. The maximum radial displacement ( $\delta_{r,\max}$ ), located on the top of the caisson

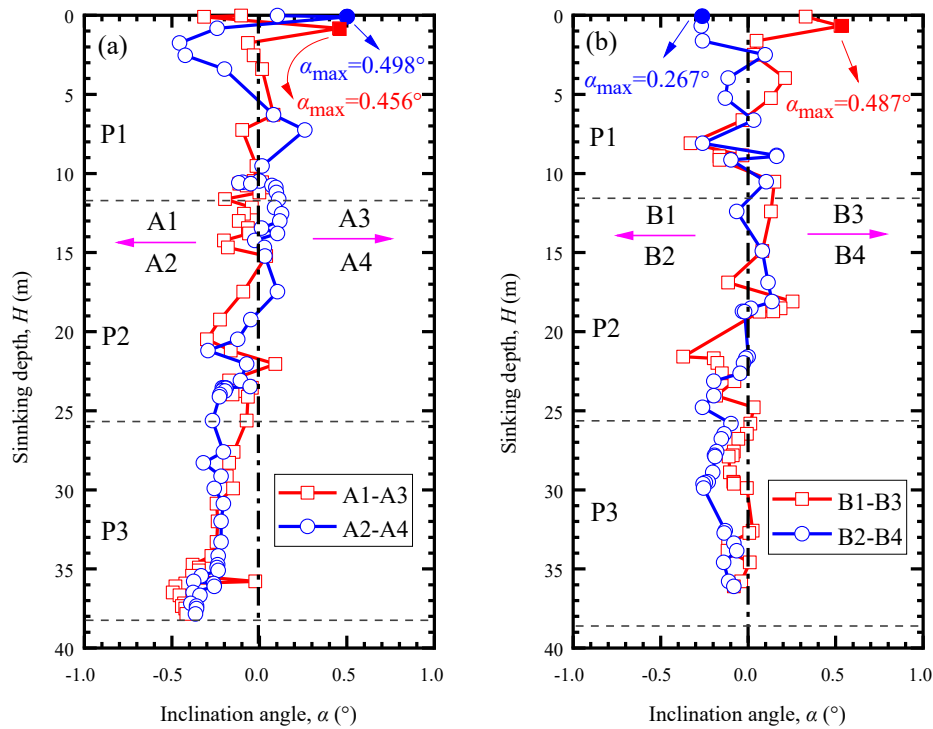


Fig. 18. Variation in inclination angles during the installation of twin LDDB caissons: (a) CA; (b) CB.

shaft, reaches 38.49 mm when finishing the installation of CB; the ratio of  $\delta_{r,max}$  to  $H$  ( $\delta_{r,max}/H$ ) at R1 is 0.099%. At R2, 5 m away from CA, the change laws of  $\delta_r$  similar to those at R1 can be found in Fig. 19(b), but the value of  $\delta_r$  at a certain depth in the same installation phase is larger due to the more obvious unloading and stress relaxation effects. The maximum radial displacement at R2 is 45.91 mm when installation of twin caissons finished, and  $\delta_{r,max}/H$  is 0.119%. Furthermore, in the earlier installation phases, the slight soil compaction effect (i.e.,  $\delta_r < 0$ ) can be found in the installation process of CA. This phenomenon can be also shown at R4 in Fig. 19(d) and R6 in Fig. 19(f). Therefore, it is concluded that, displacement modes of surrounding soils on the outsides of twin caisson shaft might be governed by soil compaction near the cutting edges in earlier installation phase; However, in the later installation phase, the displacement modes show that  $\delta_r > 0$ , which are mainly affected by the unloading and stress relaxation effect.

Monitoring points R3 and R5 are between CA and CB, the interaction between twin caissons alternately installed has a significant influence on the soils in this zone. At R3 that is 5 m away from Caisson A (i.e. 10 m away from CB), a cantilever-shaped displacement mode of soils can be observed during CA-P1 under unloading effect,  $\delta_r > 0$  can be found within installation depth in this phase; however, the soils gradually move toward CB, and  $\delta_r$  value gradually decreases as its installation begins (CB-P1), some of values in shallower ground are even lower than 0. That is, the positive and negative values of  $\delta_r$  in the shallower ground alternately occur in Phases 1 both for Caissons A and B, showing the highly complicated interaction effect, as shown in Fig. 19(c). The similar phenomenon can be observed in CA&CB-P2. The final soils' displacement profile indicates the soils at R3 still move toward CA ( $\delta_r > 0$  at R3), giving confidence that the soil displacements in this zone are mainly governed by the installation activities of adjacent caisson shafts. This so-called interaction is more clearly manifested in Fig. 19(e).

From Fig. 19(c) and (e), we have  $\delta_{r,max} = 44.40$  mm,  $\delta_{r,max}/H = 0.12\%$  at R3 and  $\delta_{r,max} = 69.85$  mm,  $\delta_{r,max}/H = 0.18\%$  at R5; implying that the more obvious geoenvironmental impacts induced by CB installation. The further observation to R6 which is 5 m away from CB [see Fig. 19(f)] and the following comparison to R2, also show the extremely obvious geoenvironmental impacts ( $\delta_{r,max} = 81.90$  mm and  $\delta_r$ ,

$\delta_{r,max} = 0.21\%$  at R6). In addition to the observed soil compaction effect in CA&CB-P1, a simple superposition effect on the radial displacement is found in Fig. 19(d), wherein  $\delta_{r,max} = 69.88$  mm and  $\delta_{r,max}/H = 0.18\%$ .

It follows from Fig. 19(a-f) that the radial displacements of soils at R1-R3 around CA are much smaller than those at R4-R6, in particular the shallower ground. This is due to the facts given as follows: (a) The CB was placed adjacent to dam of Yangzte River that have been scoured severely. The construction site was here required to be backfilled to a level ground prior to the installation, that is, the shallower ground was newly-deposited soils with the lower soil deformation modulus. (b) The tidal effect of Yangzte River had a more significant influence on the ground movement around CB than CA. Such cyclic effect also likely resulted in the reduction of soil's deformation modulus in the shallower ground.

#### 8.5. Surface settlements of existing nearby facilities

Fig. 20 illustrates variations in surface settlement ( $\delta_v$ ) at monitoring points F1, F2 and F3 of flood walls. The maximum value of surface settlement ( $\delta_{v,max}$ ) is 6.64 mm at F3, and  $\delta_{v,max}/H$  is 0.017% less than 0.15% of the design criteria provided by MOHURD. This demonstrates that the installation of twin caissons have a small influence the on surface settlements of flood walls.

Fig. 20 also describes that, in the earlier installation of twin LDDB caissons (before Mid-November 2017), the  $\delta_v$  values at F1-F3 are negative, indicating the subsidence of flood walls; meanwhile, surface settlement first increases to the maximum, then gradually restores to zero. However, in the later installation (after Mid-November 2017), the  $\delta_v$  values at F1-F3 change to be positive, showing the heave of flood walls; during this time, the heave displacement gradually increases, then slightly decreases. Such a phenomenon can be explained as: (a) The excavation-induced unloading effect and drafting effect resulted from penetration and stress-relaxation around cutting edges together caused that soils eventually move toward the centerlines of twin caisson shafts. The groundwater depression cones formed by drawdown also promote the subsidence of flood walls. (2) During the use of new installation technology in undrained stiff clays, the injection of high-pressure water,

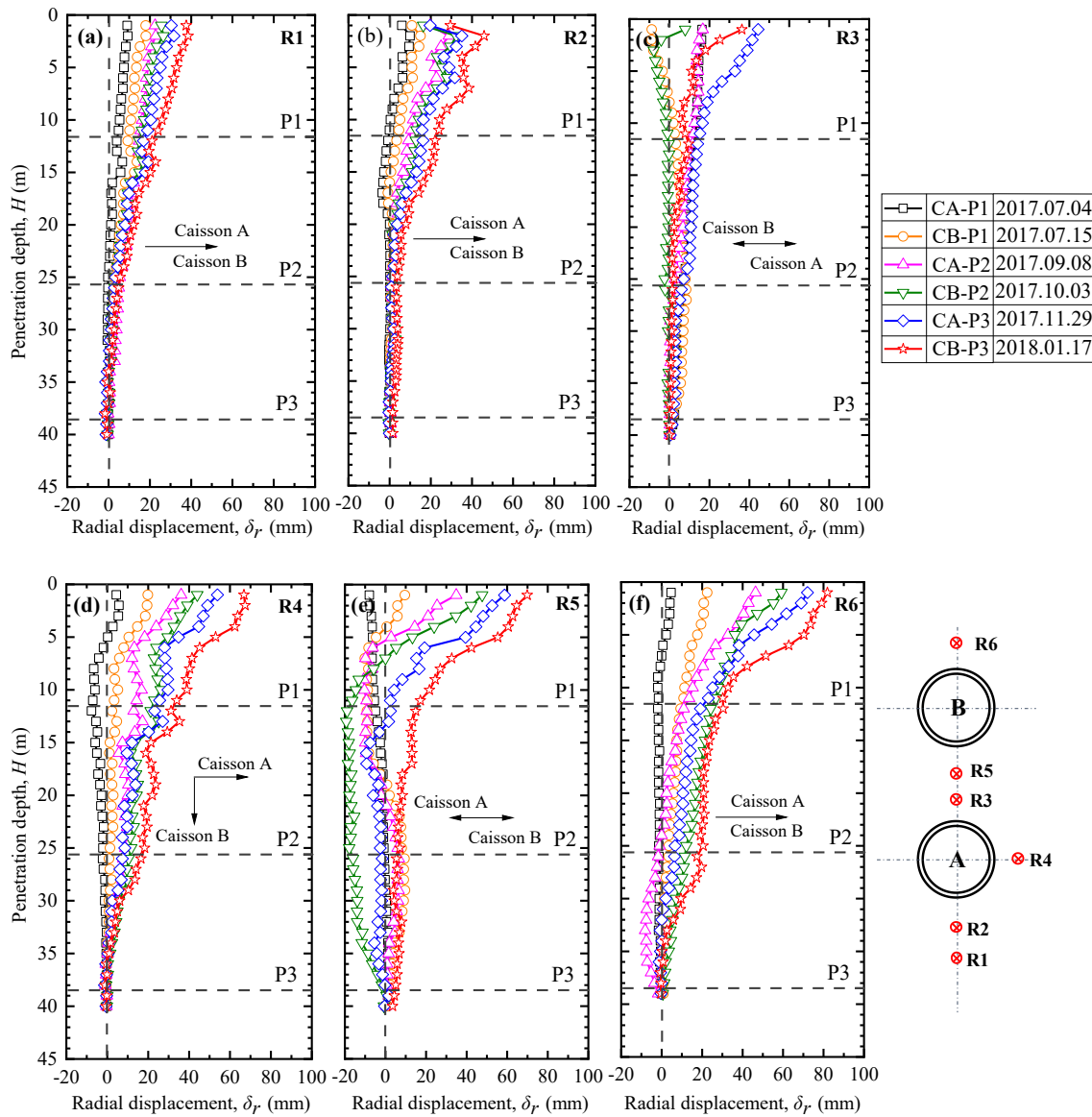


Fig. 19. Radial displacements of soils along caisson shaft induced by the installation of twin LDDB caissons at: (a) R1; (b) R2; (c) R3; (d) R4; (e) R5; (f) R6.

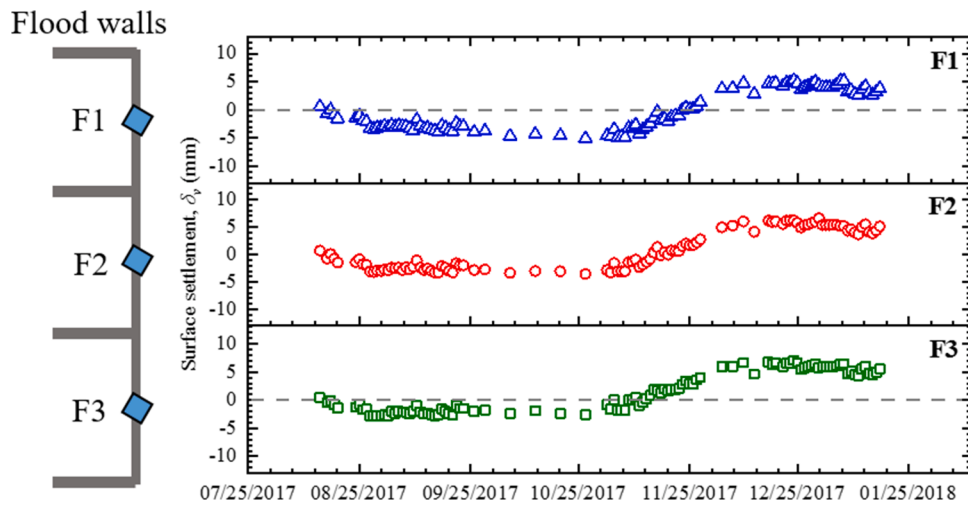


Fig. 20. Variation in surface settlements of flood walls during the installation of twin LDDB caissons.

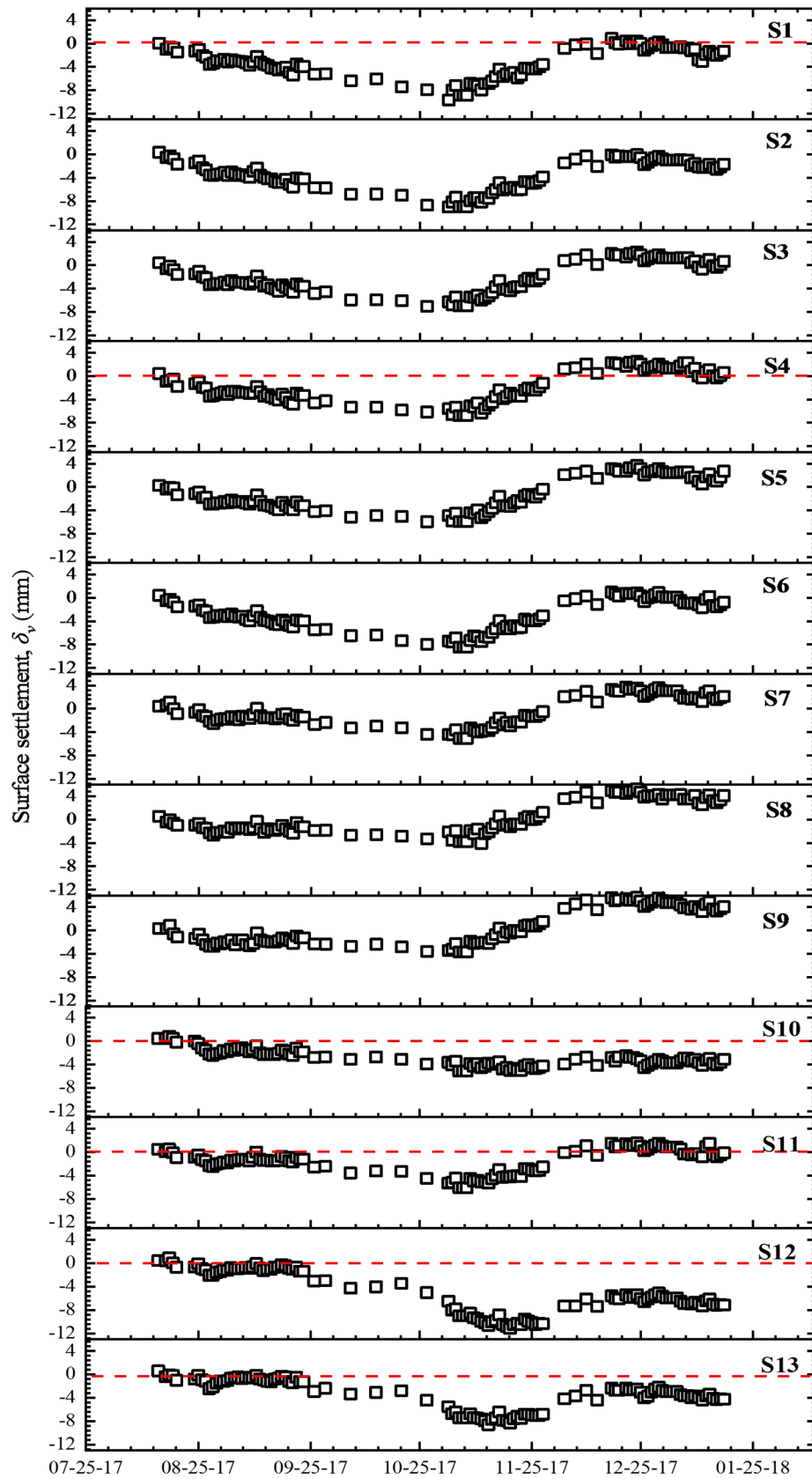


Fig. 21. Variation in surface settlements of buildings during the installation of twin LDB caissons.



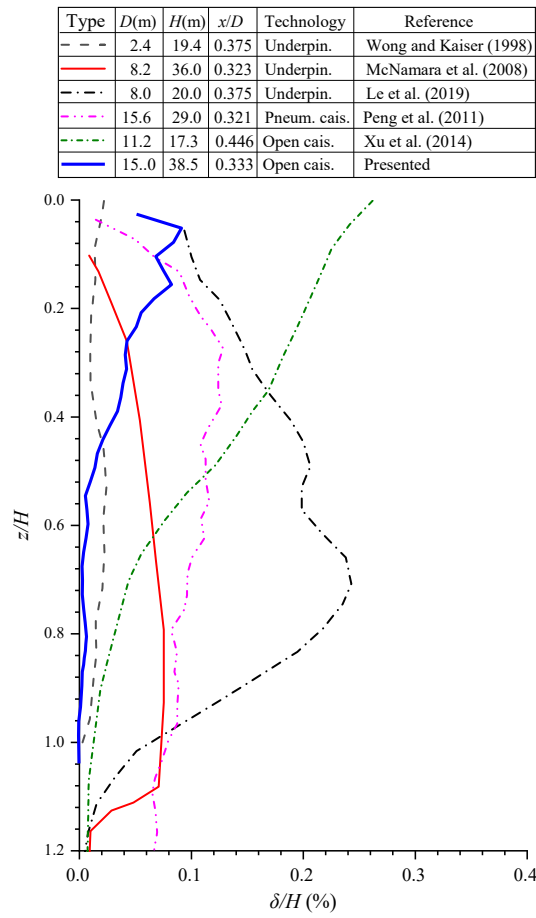


Fig. 22. Comparison of lateral displacements induced by various caisson installation technologies.

similar to the recharge of groundwater, can effectively mitigate the drawdown of groundwater and surface settlements of existing facilities; even might lead to the heave of ground.

Fig. 21 presents the variations in surface settlement ( $\delta_v$ ) at monitoring points S1-S13 of existing buildings, respectively. We can obtain that the  $\delta_{v,max}$  is 8.96 mm at S2, the  $\delta_{v,max}/H$  is 0.026% and lower than the design criteria of 0.15% (GB50007-2011, MOHURD). This further confirms that geoenvironmental impacts induced by new installation

technology are very slight. At monitoring points S1-S4 closest to twin caissons, the surface settlement induced is more sensitive. It is of interest that the observed variation laws of  $\delta_v$  at S1-S13 are similar to those at flood walls. This is closely attributed to the variation in GWL. Furthermore, the  $\delta_v$  values are lower at S10-S13, and only subsidence of existing buildings can be found due to excavation activities; showing that influential degrees of GWL on induced geoenvironmental impacts are relatively limited.

## 9. Discussion on installation effects

To assess installation effects of twin LDDB caissons using a new installation technology, a comparison of ground movements (surface and subsurface displacements) induced by various technologies is requisite. It should be pointed out that a comparison of surface ground settlement has been presented in the previous work by Lai et al. (2021) where the inaccessible surface ground settlements by field monitoring here were predicted by 3D numerical modelling. From a comparison provided by Lai et al. (2021), we confirm that the newly developed installation technology is much beneficial for limiting the surface settlement in the vicinity of the caissons.

Fig. 22 compares the profiles of normalized radial/lateral displacements ( $\delta/H$ ) at various distances ( $x/D$ ) to a caisson installed by various technologies (e.g. underpinning, pneumatic caisson-sinking, conventional open caisson-sinking and newly presented technology). The final radial displacement profile at R2 was selected for the comparison. Wong and Kaiser (1998) measured the radial displacement due to the installation of a small diameter shaft using underpinning in drained stiff silty clays. Similarly, McNamara et al. (2008) reported that a deep shaft for Crossrail was constructed by underpinning in London clay, and a secondary lining was used for the reinforcement. Le et al. (2019) experimentally studied subsurface ground movements due to the circular shaft construction using underpinning in kaolin clay, and the associated data of radial displacements were compiled here. Moreover, two rectangular caissons were installed employing pneumatic caisson-sinking (Xu et al., 2014) and conventional open caisson-sinking (Peng et al., 2011) in Shanghai soft clays, respectively. More details on the installation technologies, ground conditions and geometric configurations can be found in Table 1.

In Fig. 22, we can find that, the induced ground movements are relevant with ground conditions, the distribution of radial/lateral displacements along shafts at various  $x/D$  caused by different technologies are therefore relatively scattered. Nevertheless, the obtained  $\delta/H$  can be controlled within 0.3% for the current popular technologies reported here. The comparison with pneumatic caisson demonstrates that,

Table 1

Case histories used in this study.

No.	Reference	Data type	Location	Installation technology	Ground condition	Geometric configuration			
						D (m)	H (m)	D/H	x/D
1 <sup>a, d</sup>	Wong and Kaiser (1988)	Field observation	Edmonton, Canada	Underpinning	Sand & clay (6.5 m) Glacial matrix (13 m) Clay shale	2.8	20.0	0.140	0.375
2 <sup>a, d</sup>	McNamara et al. (2008)	Field observation	London, UK	Underpinning	London clay (30 m) Lambeth Group (18 m)	8.2	37.5	0.219	0.323
3 <sup>a, d</sup>	Le et al. (2019)	Centrifuge testing	City, Univ. of London	Underpinning	Speswhite kaolin	8.0*	20.0*	0.400	0.375
4 <sup>b, c</sup>	Peng et al. (2011)	Field observation	Shanghai, China	Pneumatic caisson	Shanghai soft soil	15.6	29.0	0.538	0.321
5 <sup>b, d</sup>	Xu et al. (2014)	Field observation	Shanghai, China	Conv. caisson sinking	Shanghai soft soil	11.2	17.3	0.647	0.446
6 <sup>a, c</sup>	This study	Field observation	Zhenjiang, China	New caisson sinking	Yangtze River floodplain deposits	15.0	38.5	0.390	0.333

\* Dimension in equivalent prototype.

<sup>a</sup> Circular caisson.

<sup>b</sup> Rectangular.

<sup>c</sup> Undrained condition.

<sup>d</sup> Drained condition.

although the interaction between twin caissons has a significant influence on induced ground movements, the newly developed open caisson sinking technology is outstanding in the aspect of limiting the geo-environmental impacts in undrained ground, as emphasized by Lai et al. (2021). The underpinning and conventional open caisson-sinking technologies in soft soils have a pronounced effect on the ground movements. For a stable and drained (dry) ground, easy-to-use underpinning still can better control the induced ground movement (Wong and Kaiser, 1988; McNamara et al. 2008). The comprehensive comparisons made here fully confirm that the new installation technology has an acceptable installation effect.

## 10. Summary and conclusions

Conventional technologies used for installation of LDDB caissons in stiff soils both under undrained and drained conditions are challenging, costly, and time-consuming. To this end, a newly developed installation technology was reported and used to install the LDDB caissons in wet ground with stiff clays. The two most significant features and advantages of this new technology are: (1) excavations in stiff soils can be performed under undrained condition using the well-structured combination between mud rushing and sucking system and stiff soil breaking system; and (2) driving forces provided by new penetration aid system can be automatically calibrated by PLC to attain the successful installation, as demonstrated in this paper and Lai et al. (2021).

Twin LDDB caissons near the bank of the Yangtze River in Zhenjiang, Southeast China were successfully sunk into undrained stiff soils first using the developed new technology. The field observation was carried out to measure the total jacking forces provided by new penetration aid system, GWL around the caisson, inclination angles of caisson shafts, radial displacements of surrounding soils and surface settlements of surrounding existing facilities, all of which are significant to ensure the installation implementation and safeguard the existing facilities. The results indicated that all the monitoring data could fall within the design criteria, demonstrating that the new technology has a better field performance. A comparison of installation effects amongst various technologies further confirm that this case yields a successful installation.

The investigation of monitoring data was undertaken to comprehensively assess the field performance, installation effects and geo-environmental impacts induced by the installation of twin LDDB caissons. Some beneficial findings can be drawn as following:

- (1) During the use of new penetration aid system, the total jacking forces increase approximately in the stepwise shape with increasing penetration depth of caisson shafts, depending on the distribution of soil layers.
- (2) The variation in GWL respectively undergoes the drawdown, stabilization and raising, which are closely to the construction behaviors of new undrained excavation method.
- (3) The more obvious but fully controllable inclinations of caisson shafts mainly occur in the earlier installation phase, the twin caisson shafts tend to incline in the same orientation due to the interaction.
- (4) The radial displacements of soils along caisson shafts are mainly affected unloading effect caused by excavation activities inside the caisson, and the radial displacements of soils between twin caissons show the very complicated interaction. Moreover, the surface settlements of surrounding existing facilities are less, and their change laws are extremely similar to those of GWL.

Although the new technology has been proven feasible, some imperfections are worth improving to facilitate its practical application in future. The more cost- and time-effective operations are also desired. Installation mechanisms of LDDB caissons during the installation appear to be unclear. Further parametric studies accounting for various operational parameters, geological conditions (e.g., GWL, stratified soils

with strong discontinuities), geometric configurations (e.g., horizontal spacing between twin caissons, penetration depth, internal diameter) are also critical to popularize the new technology. These research works need be further conducted using laboratory tests and numerical simulations. However, it might be reasonably and safely concluded that for most of LDDB caissons sunk into stiff soils, exploiting the new installation technology may constitute a promising alternative to conventional construction technology that is worth further investigation.

## Data Availability Statement

Some or all data, models, or photos generated or used during this study are available from the corresponding author by request.

## Declaration of Competing Interest

The authors declare that they have no known competing financial interests or personal relationships that could have appeared to influence the work reported in this paper.

## Acknowledgments

This study is financially supported from the National Key R&D Program of China (Grant No. 2016YFC0800201), National Natural Science Foundation of China (Grant No. 41972269), Fundamental Research Funds for the Central Universities of China (Grant No. 2242019), Postgraduate Research & Practice Innovation Program of Jiangsu Province (KYCX20\_0118) and Scientific Research Foundation of Graduate School of Southeast University (Grant No. YBPY2041). The permission of Shanghai Foundation Engineering Group Co., Ltd to report the developed technology is gratefully acknowledged. The authors are grateful to Mr. Yingwu Xu (Engineer of Shanghai Foundation Engineering Group Co., Ltd.) for his help in providing some images of Dagang waterworks project. The first author finally would like to appreciate the valuable suggestions and discussions from Dr. Jianfeng Xue at The University of New South Wales, Canberra.

## References

- Abdrabbo, F., Gaaver, K., 2012a. Challenges and uncertainties relating to open caissons. *DFI J. - J Deep Found. I.* 6 (1), 21–32.
- Abdrabbo, F.M., Gaaver, K.E., 2012b. Applications of the observational method in deep foundations. *Alexandria Eng. J.* 51 (4), 269–279.
- Allenby, D., Kilburn, D., 2015. Overview of underpinning and caisson shaft-sinking techniques. *P. I. Civil Eng.-Geotech. Eng.* 168 (1), 3–15.
- Allenby, D., Waley, G., Kilburn, D., 2009. Examples of open caisson sinking in Scotland. *P. I. Civil Eng.-Geotech. Eng.* 162 (1), 59–70.
- Belous, N., 1968. Deformation of soils and settlement of reference points at the zone where a caisson is sunk. *Soil Mech. Found. Eng.* 5 (5), 359–361.
- Bolyachevskii, B.I., Chumakov, I.S., 1975. Construction of precast open caissons with forced regulation of their sinking. *Soil Mech. Found. Eng.* 12 (6), 362–365.
- Chavda, J.T., Mishra, S., Dodagoudar, G.R., 2019. Experimental evaluation of ultimate bearing capacity of the cutting edge of an open caisson. *Int. J. Phys. Model. Geo.* 1–14.
- Cho, J., Lim, H., Jeong, S., Kim, K., 2015. Analysis of lateral earth pressure on a vertical circular shaft considering the 3D arching effect. *Tunn. Undergr. Sp. Tech.* 48, 11–19.
- Dachowski, R., Kostrzewa, P., 2017. Realization of underground objects by the open caisson method in conditions of built-up areas. *Struct. Environ.* 9 (5), 215–223.
- Dhinian, R., 2003. Caisson Sickness During Pneumatic Sinking, Role of Concrete Bridges in Sustainable Development: Proceedings of the International Symposium held at the University of Dundee, Scotland, UK on 3–4 September 2003. Thomas Telford Publishing, pp. 361–368.
- Fischer, G.R., Gerszewski, W.L., Barchok, F.J., Yavarow, M.K., 2004. Deep Caisson Sinking in Soft Soils, Grand Forks, North Dakota, Fifth International Conference on Case Histories in Geotechnical Engineering. Missouri University of Science and Technology, New York, USA.
- Georgiannou, V.N., Serafis, A., Pavlopoulou, E.-M., 2017. Analysis of a vertical segmental shaft using 2D & 3D finite element codes. *Int. J. GEOMATE* 13 (36), 138–146.
- Ho, C.E., 2002. Settlement Performance of Large Diameter Friction Caissons in Boulderly Clay, Deep Foundations 2002: An International Perspective on Theory, Design, Construction, and Performance, pp. 525–541.
- Hoffman, J., Roboski, J., Finno, R.J., 2004. Ground movements caused by caisson installation at the Lurie Excavation project. *Geotech. Eng. Transp. Projects* 1280–1289.

- Hong, W.-P., Yea, G.-G., Kim, T.-H., Nam, J.-M., 2005. Evaluation of unit skin friction to large size pneumatic caisson during the process of sinking. In: The Fifteenth International Offshore and Polar Engineering Conference. International Society of Offshore and Polar Engineers.
- Jiang, B.-N., Ma, J.-L., Chu, J.-L., 2019a. The influence of soil surrounding the caisson cutting edge to excavation and sinking. In: IACGE 2018: Geotechnical and Seismic Research and Practices for Sustainability. ASCE, Chongqing, China.
- Jiang, B.-N., Wang, M.-T., Chen, T., Zhang, L.-L., Ma, J.-L., 2019b. Experimental study on the migration regularity of sand outside a large, deep-water, open caisson during sinking. *Ocean Eng.* 193, 106601.
- Khasawneh, Y.A., Al-Omari, A.A., Sharo, A.A., 2017. Distress of a large diameter underground reinforced concrete shaft. *Congr. Tech. Adv.* 2017, 184–196.
- Kim, K.-Y., Lee, D.-S., Cho, J., Jeong, S.-S., Lee, S., 2013. The effect of arching pressure on a vertical circular shaft. *Tunn. Undergr. Sp. Tech.* 37, 10–21.
- Kumar, N.D., Rao, S.N., 2010. Earth pressures on caissons in marine clay under lateral loads—a laboratory study. *Appl. Ocean Res.* 32 (1), 58–70.
- Lai, F., Liu, S., Deng, Y., Sun, Y., Wu, K., Liu, H., 2020. Numerical investigations of the installation process of giant deep-buried circular open caissons in undrained clay. *Comput. Geotech.* 118, 103322.
- Lai, F., Zhang, N., Liu, S., Sun, Y., Li, Y., 2021. Ground movements induced by installation of twin large diameter deeply-buried caissons: 3D numerical modeling. *Acta Geotech.* 16, 2933–2961.
- Le, B.T., Goodey, R.J., Divall, S., 2019. Subsurface ground movements due to circular shaft construction. *Soils Found.* 59 (5), 1160–1171.
- Li, C., Lai, F., Huang, H., 2022. Numerical Investigation of Ground Settlements Induced by Installation of Large Diameter Deeply-Buried Caissons in Undrained Clays. *Soil Mechanics and Foundation Engineering* 58 (6), 511–517.
- Liu, F., 2014. Lateral earth pressures acting on circular retaining walls. *Int. J. Geomech.* 14 (3), 04014002.
- Maslik, V., Kiselev, V., Chizhov, I., 1978. New method of sinking open caissons in a double thixotropic jacket. *Soil Mech. Found. Eng.* 15 (2), 98–99.
- McNamara, A., Roberts, T., Morrison, P., Holmes, G., 2008. Construction of a deep shaft for Crossrail. *P. I. Civil Eng.-Geotech Eng.* 161, 299–309.
- Ministry of Housing and Urban and Rural Development of the People's Republic of China (MOHURD), 2011. Code for design of building foundation. China Architecture & Building Press, Beijing, China.
- Morrison, P., McNamara, A., Roberts, T., 2004. Design and construction of a deep shaft for Crossrail. *P. I. Civil Eng.-Geotech.* 157 (4), 173–182.
- Newman, T., Wong, H.-Y., 2011. Sinking a jacked caisson within the London Basin geological sequence for the Thames Water Ring Main extension. *Q. J. Eng. Geol. Hydroge.* 44 (2), 221–232.
- Peng, F.-L., Dong, Y.-H., Wang, H.-L., Jia, J.-W., Li, Y.-L., 2019. Remote-control technology performance for excavation with pneumatic caisson in soft ground. *Automat. Constr.* 105, 102834.
- Peng, F.-L., Wang, H.-L., Tan, Y., Xu, Z.-L., Li, Y.-L., 2011. Field measurements and finite-element method simulation of a tunnel shaft constructed by pneumatic caisson method in Shanghai soft ground. *J. Geotech. Geoenviron. Eng.* 137 (5), 516–524.
- Royston, R., 2018. Investigation of Soil-structure Interaction for Large Diameter Caissons. University of Oxford, Oxford.
- Royston, R., Phillips, B.M., Sheil, B.B., Byrne, B., 2016. Bearing Capacity Beneath Tapered Blades of Open Dug Caissons in Sand. Civil Engineering Research in Ireland. Civil Engineering Research Association of Ireland, Dublin, Ireland.
- Royston, R., Sheil, B.B., Byrne, B.W., 2021. Undrained bearing capacity of the cutting face for an open caisson. *Géotechnique* 1–10.
- Schwamb, T., 2014. Performance Monitoring and Numerical Modelling of a Deep Circular Excavation. University of Cambridge, Cambridge.
- Sheil, B., Royston, R., Byrne, B., 2018. Real-time monitoring of large-diameter caissons. In: Proceedings of China-Europe Conference on Geotechnical Engineering. Springer, pp. 725–729.
- Shanghai Municipal Engineering Design Institute (SMEDI), 2015. Specification for Structural Design of Reinforced Concrete Sinking Well of Water Supply and Sewerage Engineering. China Planning Press, Beijing, China.
- Solov'ev, N., 2008. Use of limiting-equilibrium theory to determine the bearing capacity of soil beneath the blades of caissons. *Soil Mech. Found. Eng.* 45 (2).
- Spagnoli, G., Oreste, P., Lo Bianco, L., 2017. Estimation of shaft radial displacement beyond the excavation bottom before installation of permanent lining in nondilatant weak rocks with a novel formulation. *Int. J. Geomech.* 17 (9), 04017051.
- Sun, Y., Shen, S., Xu, Z., Xia, X., 2014. Prediction of lateral displacement of soil behind the reaction wall caused by pipe jacking operation. *Tunn. Undergr. Sp. Tech.* 40, 210–217.
- Sun, Y., Su, J.-B., Xia, X.-H., Xu, Z.-L., 2015. Numerical analysis of soil deformation behind the reaction wall of an open caisson induced by horizontal parallel pipe-jacking construction. *Can. Geotech. J.* 52 (12), 2008–2016.
- Sun, Y., Wu, F., Sun, W., Li, H., Shao, G., 2019. Two underground pedestrian passages using pipe jacking: case study. *J. Geotech. Geoenviron. Eng.* 145 (2), 05018004.
- Tobar, T., Meguid, M.A., 2010. Comparative evaluation of methods to determine the earth pressure distribution on cylindrical shafts: a review. *Tunn. Undergr. Sp. Tech.* 25 (2), 188–197.
- Tomlinson, M.J., Boorman, R., 2001. Foundation Design and Construction. Pearson Education, New York.
- Umeda, N., Fujii, N., Inoue, T., Ohuchi, M., Shimoma, M., Tamura, T., 2006. Numerical modeling of pneumatic caisson method. *J. Appl. Mech.* 9, 603–612.
- Verstov, V., Gaido, A., Yudina, A., Kolchedantsev, L., 2019. New technology for soil extraction when sinking open caissons. In: *Geotechnics Fundamentals and Applications in Construction: New Materials, Structures, Technologies and Calculations*, pp. 402–409.
- Wong, R., Kaiser, P., 1988. Behaviour of vertical shafts: reevaluation of model test results and evaluation of field measurements. *Can. Geotech. J.* 25 (2), 338–352.
- Xu, P., Li, Y., Xu, W., 2014. Field measurement and analysis of influence of jacked open caisson construction on environments. *Rock Soil Mech.* 35 (4), 1084–1094.
- Yan, F.Y., Guo, Y.C., Liu, S.Q., 2011. The bearing capacity analyses of soil beneath the blade of circular caisson. *Adv. Mater. Res.* 250, 1794–1797.
- Yao, Q., Yang, X., Li, H., 2014. Construction technology of open caisson for oversize surge shaft in drift gravel stratum. *Electr. J. Geotech. Eng.* 19, 5725–5738.
- Yea, G.-G., Kim, T.-H., 2012. Vertical cutting edge forces measured during the sinking of pneumatic caisson. *Mar. Georesour. Geotechnol.* 30 (2), 103–121.
- Yea, G.-G., Kim, T.-H., Kang, G.-C., 2015. Assessing unit skin friction of pneumatic caissons. *Mar. Georesour. Geotechnol.* 33 (2), 127–134.
- Zhao, G., Meng, S., Guan, C., Yang, Y., 2019. Test study on the stress and deformation behaviors of a shaft supported by a prefabricated prestressed structure. *Appl. Sci.-Basel* 9 (4), 629.
- Zhao, X., Xu, J., Mu, B., Li, B., 2015. Macro-and meso-scale mechanical behavior of caissons during sinking. *J. Test. Eval.* 43 (2), 1–13.
- Zheng, W., Tao, F., Guangxiu, F., 2019. Study of the construction technology of caisson under complex geological conditions. *J. Phys.: Conf. Series. IOP Publishing*, 022063.
- Zou, H., Liu, S., Cai, G., Puppala, A.J., Bheemasetti, T.V., 2017. Multivariate correlation analysis of seismic piezocone penetration (SCPTU) parameters and design properties of Jiangsu quaternary cohesive soils. *Eng. Geol.* 228, 11–38.